INTERNATIONAL JOURNAL FOR NUMERICAL METHODS IN ENGINEERING
Int. J. Numer. Meth. Engng 2005; **62**:1264–1294
Published online 1 December 2004 in Wiley InterScience (www.interscience.wiley.com). DOI: 10.1002/nme.1217

Smart element method I. The Zienkiewicz–Zhu feedback

Shaofan Li*,†, Xiaohu Liu and Anurag Gupta

Department of Civil and Environmental Engineering, University of California, Berkeley, CA94720, U.S.A.

SUMMARY

A new error control finite element formulation is developed and implemented based on the variational multiscale method, the inclusion theory in homogenization, and the Zienkiewicz–Zhu error estimator. By synthesizing variational multiscale method in computational mechanics, the equivalent eigenstrain principle in micromechanics, and the Zienkiewicz–Zhu error estimator in the finite element method (FEM), the new finite element formulation can automatically detect and subsequently homogenize its own discretization errors in a self-adaptive and a self-adjusting manner. It is the first finite element formulation that combines an optimal feedback mechanism and a precisely defined homogenization procedure to reduce its own discretization errors and hence to control numerical pollutions.

The paper focuses on the following two issues: (1) how to combine a multiscale method with the existing finite element error estimate criterion through a feedback mechanism, and (2) convergence study. It has been shown that by combining the proposed variational multiscale homogenization method with the Zienkiewicz–Zhu error estimator a clear improvement can be made on the coarse scale computation. It is also shown that when the finite element mesh is refined, the solution obtained by the variational eigenstrain multiscale method will converge to the exact solution.

KEY WORDS: eigenstrain method; homogenization; micromechanics; variational multiscale method; Zienkiewicz–Zhu criterion

1. INTRODUCTION

Recently, the present authors [1] proposed a so-called variational eigenstrain multiscale method as a self-adaptive finite element method that distinguishes itself from the h-adaptive finite element method (FEM), the p-adaptive finite element method, and the h–p finite element method.

*Correspondence to: S. Li, Department of Civil and Environmental Engineering, University of California, Berkeley, CA94720, U.S.A.
†E-mail: li@ce.berkeley.edu

Contract/grant sponsor: NSF; contract/grant number: CMS-0239130

Received 5 January 2004
Revised 15 April 2004
Accepted 19 July 2004

The existing adaptive solutions for FEM are: (1) refining an FEM mesh to reduce the discretization error, or (2) increasing the polynomial degree of an FEM interpolant field to increase interpolation accuracy, which, in turn, improve results of the FEM computations.

The proposed variational eigenstrain multiscale method is based on an entirely different philosophy. To achieve the same goal, the new multiscale method attempts to reduce the discretization error without refining the mesh and without changing the interpolation field, instead it attains a better numerical accuracy through a feedback mechanism to modify the original weak formulation, to homogenize and hence alleviate the numerical error. In doing so, the proposed method obtains an improvement in one step. This distinguishes the proposed method from traditional adaptive methods, which need a series of solutions. Because of its feedback and self-adapting nature, we take the liberty to call the method as '*smart element method*'.

In general, any discretization of a continuum will produce a discretization error distribution over the domain of interest. This discretization error may be measured by the residue of coarse scale solution.

Intuitively, a discrete weak formulation with a uniform distribution of the discretization error may produce better numerical results than those with a non-uniform discretization error distribution, because the gradient of a uniform discretization error will vanish. In practice, it is almost impossible to find a problem with uniform discretization error distribution, because it depends on the mesh construction, the configuration of the domain, and the boundary value problem itself.

The basic idea of the smart element method is that one can build a numerical error control algorithm by homogenizing the discretization error in a given mesh, to achieve a better computational accuracy in a coarse scale computation.

To homogenize the discretization error, the effect of the residue of coarse scale solution is considered to be equivalent to that of a fictitious eigenstrain distribution. We then solve the fine scale boundary value problem analytically without discretization, and the effect of discretization error of coarse scale is translated into an equivalent eigenstrain distribution, which becomes the 'body force' of the fine scale (disturbance) solution.

To correct the coarse scale error distribution, we adjust the original coarse weak formulation to compensate the error disturbance due to the discretization, or in other words, we are looking for an effective stiffness matrix that homogenizes the discretization error. To illustrate the principle of the smart element method, we choose two-dimensional (2D) elasticity as a model problem. We homogenize the discretization error by first solving the fine scale disturbance analytically (with certain assumptions and approximations), and then incorporate it into the coarse scale discrete formulation, so that one can construct a self-adjusting, or a 'smart' weak formulation, which is capable to reduce its own discretization error accordingly.

It is worth noting that in late 1970s, Cantin *et al*. [2] devised a feedback mechanism to calculate smooth displacement gradients using a procedure of successive iteration. In this work, we solve the fine scale solution analytically by utilizing the Eshelby's eigenstrain formulation and the single inclusion solution [3–5] in a single step. An analytical expression of the fine scale solution is the key feature of our formulation. Substituting the analytical estimate of fine scale solution into the coarse scale weak formulation, one can find a homogenized coarse scale weak form, and subsequently, one can solve the homogenized coarse scale problem and obtain a numerical solution with better accuracy.

In this part of the work, we focus our attention upon following two issues: (1) how to combine the newly proposed variational eigenstrain multiscale method with the existing finite

element error estimate criterion, and (2) study of the convergence property of the variational eigenstrain multiscale method.

It should be noted that the multiscale homogenization method proposed in this paper is different from the widely spread *asymptotic multiscale homogenization methods* (e.g. References [6–8], and many others). There are no physical inhomogeneities involved in the problems discussed here. The fictitious inhomogeneities (eigenstrains) are numerical errors due to mesh discretization. By homogenizing the discretization error, we hope to achieve better accuracy without much additional computational cost.

In Section 2, we shall first review the variational eigenstrain multiscale formulation. In Section 3, we shall discuss on how to incorporate the Zienkiewicz–Zhu error estimator [9–11] into the variational eigenstrain multiscale formulation [12–14]. The convergence of the method is examined in Section 4, and a few remarks are being made in Section 5.

2. VARIATIONAL EIGENSTRAIN MULTISCALE FORMULATION

We first review the variational eigenstrain multiscale formulation in the context of linear elasticity theory [12, 14].

Consider a simply connected domain, $\Omega \in \mathbb{R}^d$ (d is the dimension of the physical space). Displacement boundary conditions and traction boundary conditions are prescribed on the boundary of $\Gamma_u \cup \Gamma_t = \partial\Omega$ and $\Gamma_u \cap \Gamma_t = \emptyset$. We are interested in the following boundary-value problem of elastostatics:

$$\sigma_{ji,j} + b_i = 0 \quad \forall \mathbf{x} \in \Omega \tag{1}$$

$$u_i = u_i^0 \quad \forall \mathbf{x} \in \Gamma_u \tag{2}$$

$$\sigma_{ij} n_j = t_i^0 \quad \forall \mathbf{x} \in \Gamma_t \tag{3}$$

where b_i is the body force, u_i is the displacement component, n_j is the outward-normal of the displacement boundary, u_i^0 is the prescribed displacement field, and t_i^0 is the prescribed traction vector. The Cauchy stress components, σ_{ij}, are linked with the infinitesimal strain components by the generalized Hooke's law,

$$\sigma_{ij} = C_{ijk\ell}\varepsilon_{k\ell}$$

where $C_{ijk\ell}$ is the elastic tensor. The infinitesimal strain is defined as the symmetric part of displacement gradient,

$$\varepsilon_{ij} = u_{(i,j)} = \tfrac{1}{2}(u_{i,j} + u_{j,i})$$

Define the trial function and the test function spaces,

$$\mathscr{S} = \{\mathbf{u}(\mathbf{x}) | \mathbf{u}(\mathbf{x}) \in [H^1(\Omega)]^d, \mathbf{u} = \mathbf{u}^0, \ \forall \mathbf{x} \in \Gamma_u\} \tag{4}$$

$$\mathscr{V} = \{\mathbf{w}(\mathbf{x}) | \mathbf{w}(\mathbf{x}) \in [H^1(\Omega)]^d, \mathbf{w} = \mathbf{0}, \ \forall \mathbf{x} \in \Gamma_u\} \tag{5}$$

Note that standard notations in functional analysis (e.g. Reference [15] or [16]) are used here without elaboration.

The variational statement of the above boundary-value problem is

Find $\mathbf{u} \in \mathscr{S}$ *such that*

$$\int_\Omega w_{(i,j)} C_{ijk\ell} u_{(k,\ell)} \, \mathrm{d}\Omega = \int_\Omega w_i b_i \, \mathrm{d}\Omega + \int_{\Gamma_t} w_i t_i^0 \, \mathrm{d}S \quad \forall \mathbf{w} = w_i \mathbf{e}_i \in \mathscr{V} \tag{6}$$

Define a bi-linear form

$$a(\mathbf{w}, \mathbf{u}) \colon \ \mathscr{V} \times \mathscr{S} \to \mathbb{R}, \quad a(\mathbf{w}, \mathbf{u}) := \int_\Omega (\nabla \otimes \mathbf{w}) : \mathbf{C} : (\nabla \otimes \mathbf{u}) \, \mathrm{d}\Omega \tag{7}$$

and two linear forms

$$(\mathbf{w}, \mathbf{b})_\Omega \colon \ \mathscr{V} \times [H^{-1}(\Omega)]^d \to \mathbb{R}, \quad (\mathbf{w}, \mathbf{b})_\Omega := \int_\Omega \mathbf{w} \cdot \mathbf{b} \, \mathrm{d}\Omega \tag{8}$$

$$(\mathbf{w}, \mathbf{t})_{\Gamma_t} \colon \ \mathscr{V} \times [H^{1/2}(\Omega)]^d \to \mathbb{R}, \quad (\mathbf{w}, \mathbf{t})_{\Gamma_t} := \int_{\Gamma_t} \mathbf{w} \cdot \mathbf{t} \, \mathrm{d}S \tag{9}$$

We can then rewrite the weak form (6) as

$$a(\mathbf{w}, \mathbf{u}) = (\mathbf{w}, \mathbf{b})_\Omega + (\mathbf{w}, \mathbf{t}^0)_{\Gamma_t} \quad \forall \mathbf{w} \in \mathscr{V} \tag{10}$$

2.1. Two-scale formulation

Following Hughes *et al.* [14], we assume that the solution of the weak form (10) can be decomposed into two solutions with different spatial resolutions, i.e.

$$\mathbf{u} = \bar{\mathbf{u}} + \mathbf{u}' \tag{11}$$

$$\mathbf{w} = \bar{\mathbf{w}} + \mathbf{w}' \tag{12}$$

where $\bar{\mathbf{u}}$ and $\bar{\mathbf{w}}$ represent the coarse scale solution and the corresponding conjugate coarse scale solution; whereas $\mathbf{u}'$ and $\mathbf{w}'$ represent the fine scale solution and the corresponding conjugate fine scale solution.

Accordingly, we can decompose the trial function space and the test function space into the direct sum of a coarse scale space and a fine scale space, i.e. $\mathscr{S} = \bar{\mathscr{S}} \oplus \mathscr{S}'$ and $\mathscr{V} = \bar{\mathscr{V}} \oplus \mathscr{V}'$. Since we are going to solve $\bar{\mathbf{u}}$ numerically and $\mathbf{u}'$ analytically, $\bar{\mathscr{S}}$ and $\bar{\mathscr{V}}$ are finite dimensional spaces, whereas $\mathscr{S}'$ and $\mathscr{V}'$ are infinite-dimensional.

We adopt the assumptions made by Hughes *et al.* [14] on the boundary,

$$\bar{\mathbf{u}}(\mathbf{x}) = \mathbf{u}_0, \ \ \forall \mathbf{x} \in \Gamma_u, \quad \text{and} \quad \bar{\mathbf{u}} \in \bar{\mathscr{S}} \tag{13}$$

$$\mathbf{u}'(\mathbf{x}) = 0, \ \ \forall \mathbf{x} \in \Gamma_u, \quad \text{and} \quad \mathbf{u}' \in \mathscr{S}' \tag{14}$$

$$\bar{\mathbf{w}}(\mathbf{x}) = 0, \ \ \forall \mathbf{x} \in \Gamma_u, \quad \text{and} \quad \bar{\mathbf{w}} \in \bar{\mathscr{V}} \tag{15}$$

$$\mathbf{w}'(\mathbf{x}) = 0, \ \ \forall \mathbf{x} \in \Gamma_u, \quad \text{and} \quad \mathbf{w}' \in \mathscr{V}' \tag{16}$$

The weak form (10) then becomes

$$a(\bar{\mathbf{w}} + \mathbf{w}', \bar{\mathbf{u}} + \mathbf{u}') = (\bar{\mathbf{w}} + \mathbf{w}', \mathbf{b})_\Omega + (\bar{\mathbf{w}} + \mathbf{w}', \mathbf{t}^0)_{\Gamma_t}$$

Since $\bar{\mathbf{w}}$ and $\mathbf{w}'$ are independent, one can obtain the weak formulation at different scales, i.e.

$$a(\bar{\mathbf{w}}, \bar{\mathbf{u}}) + a(\bar{\mathbf{w}}, \mathbf{u}') = (\bar{\mathbf{w}}, \mathbf{b})_\Omega + (\bar{\mathbf{w}}, \mathbf{t}^0)_{\Gamma_t} \quad \forall \bar{\mathbf{w}} \in \bar{\mathscr{V}} \tag{17}$$

$$a(\mathbf{w}', \bar{\mathbf{u}}) + a(\mathbf{w}', \mathbf{u}') = (\mathbf{w}', \mathbf{b})_\Omega + (\mathbf{w}', \mathbf{t}^0)_{\Gamma_t} \quad \forall \mathbf{w}' \in \mathscr{V}' \tag{18}$$

If we assume that the linear form between the fine scale test function and the prescribed traction vector is negligible, i.e.

$$(\mathbf{w}', \mathbf{t}^0)_{\Gamma_t} = 0$$

Then it is not difficult to show that the solution of weak form (18) is the weak solution of the following boundary value problem (e.g. Reference [17])

$$C_{ijk\ell} u'_{k,\ell j} + C_{ijk\ell} \bar{u}_{k,\ell j} + b_i = 0 \quad \forall \mathbf{x} \in \Omega \tag{19}$$

$$u'_i = 0 \quad \forall \mathbf{x} \in \Gamma_u \tag{20}$$

$$\sigma'_{ij} n_j = 0 \quad \forall \mathbf{x} \in \Gamma_t \tag{21}$$

where σ'_{ij} are the stresses in the fine scale, and the term $\bar{R}_i = C_{ijk\ell} \bar{u}_{k,\ell} + b_i \neq 0$ is the residual of the coarse scale solution, or the residual of the resolved scale, which will not be zero since coarse scale numerical solution is not the exact solution.

To facilitate the presentation, we first outline the general idea or philosophy of the proposed method. We view the residual as the effect of an equivalent eigenstrain field, i.e.

$$\bar{R}_i = C_{ijk\ell} \bar{u}_{k,\ell j} + b_i =: -C_{ijk\ell} \varepsilon^*_{k\ell,j} \tag{22}$$

It is worth noting that if the body force in the above equation equals zero, the eigenstrain will be the negative coarse scale strain.

We may consider the fine scale displacement field as the disturbance field driven by the residual of the coarse scale displacement field. By solving the BVP (19)–(21), we may be able to express the fine scale solution in terms of the residual of the coarse scale solution. Using the techniques in micromechanics (e.g. Reference [18]), we attempt to utilize Eshelby's equivalent inclusion theory to express a subgrid fine scale correction due to the discretization error of a coarse scale computation. In principle, this fine scale solution of Equations (19)–(21) may be solved and be expressed in a general form

$$u'_{(i,j)}(\mathbf{x}) = S_{ijk\ell} \circ \varepsilon^*_{k\ell} \tag{23}$$

At this point, $S_{ijk\ell}$ is viewed as an abstract transformation operator, which may depend on the spatial location.

After finding the fine scale solution, one can substitute (23) into the equilibrium equation, and obtain the following equilibrium equation:

$$[C_{ijk\ell}(\bar{u}_{(k,\ell)} + S_{k\ell mn} \circ \varepsilon^*_{mn})]_{,j} + b_i = 0 \tag{24}$$

Because ε^*_{ij} are related with $\bar{u}_{(i,j)}$, we may eventually find a homogenized elastic tensor, $C^{\mathrm{H}}_{ijk\ell}$, and a homogenized body force, b^{H}_i, which then allow us to derive a homogenized equilibrium equation at coarse scale,

$$[C^{\mathrm{H}}_{ijk\ell}\bar{u}_{(k,\ell)}]_{,j} + b^{\mathrm{H}}_i = 0 \tag{25}$$

together with the boundary conditions,

$$\bar{u}_i = u^0_i \quad \forall \mathbf{x} \in \Gamma_u \tag{26}$$

$$\bar{\sigma}_{ji} n_j = t^0_i \quad \forall \mathbf{x} \in \Gamma_t \tag{27}$$

where $\bar{\sigma}_{ij} = C_{ijk\ell}\bar{u}_{(k,\ell)}$ is the coarse scale stress.

After homogenization, the corresponding coarse scale weak problem becomes,

Find $\bar{\mathbf{u}} \in \mathscr{S}$ *such that*

$$\int_\Omega \bar{w}_{(i,j)} C^{\mathrm{H}}_{ijk\ell}\bar{u}_{(k,\ell)}\,\mathrm{d}\Omega = \int_\Omega \bar{w}_i b^{\mathrm{H}}_i\,\mathrm{d}\Omega + \int_{\Gamma_t} \bar{w}_i t^{\mathrm{H}}_i\,\mathrm{d}S \quad \forall \bar{\mathbf{w}} = \bar{w}_i \mathbf{e}_i \in \mathscr{V} \tag{28}$$

To sum it up, the objective of the new method is to find the homogenized elastic stiffness tensor or the corresponding finite element stiffness matrix, and to replace the initial coarse scale weak formulation with the homogenized weak formulation (28), which has the ability to adjust the discretization error automatically. By doing so, it is believed that the coarse scale solution of the homogenized weak formulation (28) could be more accurate than the naive coarse scale solution of (6) with virtually no additional computational cost.

In contrast to the early version of the variational multiscale method, the proposed variational eigenstrain multiscale method solves the fine scale solution analytically, or approximates the fine scale solution analytically. There are several different approaches to obtain the fine scale solution (see Reference [1]). In what follows, we focus on how to use Eshelby's single inclusion solution, i.e. the Eshelby tensor for a circular inclusion, and the Zienkiewicz–Zhu recovery procedure to find the fine scale solution.

3. FINE SCALE SOLUTION VIA THE ZIENKIEWICZ–ZHU FEEDBACK

3.1. Fine scale solution

To obtain the fine scale solution, we exploit the Somigliana identity [19], which gives an integral representation of the fine scale solution (19)–(21):

$$\begin{aligned} u'_i(\mathbf{y}) = &\int_\Omega (C_{mnk\ell}\bar{u}_{k,\ell n}(\mathbf{x}) + b_m(\mathbf{x}))G^\infty_{im}(\mathbf{y}-\mathbf{x})\,\mathrm{d}\Omega_x \\ &+ \int_{\partial\Omega} \sigma'_{mn}(\mathbf{x})n_n(\mathbf{x})G^\infty_{im}(\mathbf{y}-\mathbf{x})\,\mathrm{d}S_x + \int_{\partial\Omega} \sigma^{G^\infty_i}_{k\ell}(\mathbf{y}-\mathbf{x})n_\ell u'_k(\mathbf{x})\,\mathrm{d}S_x \end{aligned} \tag{29}$$

where $G^{\infty}_{im}(\mathbf{y}-\mathbf{x})$ is Green's function for linear elasticity in an infinite domain, $\sigma^{G^{\infty}_i}_{k\ell}$ is the stress of Green's function, and n_ℓ is the out-normal of the surface, $\partial\Omega$. The subscript x in the term $\mathrm{d}\Omega_x$ and $\mathrm{d}S_x$ of the above equation denotes the fact that the integral is evaluated with respect to the variable $\mathbf{x}$.

According to the boundary conditions (20) and (21), the above equation reduces to

$$u'_i(\mathbf{y}) = \int_\Omega (C_{mnk\ell}\bar{u}_{k,\ell n}(\mathbf{x}) + b_m(\mathbf{x}))G^{\infty}_{im}(\mathbf{y}-\mathbf{x})\,\mathrm{d}\Omega_x + \int_{\Gamma_u} \sigma'_{mn}(\mathbf{x})n_n G^{\infty}_{im}(\mathbf{y}-\mathbf{x})\,\mathrm{d}S_x + \int_{\Gamma_t} \sigma^{G^{\infty}_i}_{k\ell}(\mathbf{y}-\mathbf{x})n_\ell u'_k(\mathbf{x})\,\mathrm{d}S_x \tag{30}$$

Since the fine scale solution is only driven by the residual of the coarse scale solutions and if we assume that all boundary conditions can be enforced exactly at coarse scale level, one may expect that the resolution of the exact solution at the boundary can be resolved by using coarse scale solution only. Therefore, we postulate that all the boundary contributions from the fine scale solution are small, and we adopt the following approximations:

$$\text{A1.} \quad \int_{\Gamma_u} \sigma'_{ij}(\mathbf{x})n_j(\mathbf{x})G^{\infty}_{im}(\mathbf{y}-\mathbf{x})\,\mathrm{d}S_x \approx 0 \tag{31}$$

$$\text{A2.} \quad \int_{\Gamma_t} \sigma^{G^{\infty}_m}_{k\ell}(\mathbf{y}-\mathbf{x})n_\ell(\mathbf{x})u'_k(\mathbf{x})\,\mathrm{d}S_x \approx 0 \tag{32}$$

In passing, we note that if coarse scale solution satisfies all the boundary condition, i.e.

$$\bar{\mathbf{u}} = \mathbf{u}^0 \quad \forall \mathbf{x} \in \Gamma_u \tag{33}$$

$$\bar{\boldsymbol{\sigma}} \cdot \mathbf{n} = \mathbf{t}^0 \quad \forall \mathbf{x} \in \Gamma_t \tag{34}$$

One may assume that the fine scale displacement fields and stress fields are oscillating along the boundary $\partial\Omega$ such that

$$\oint_{\partial\Omega} \sigma'_{ij}n_j\,\mathrm{d}S_x \approx 0 \quad \text{and} \quad \oint_{\partial\Omega} u'_k\,\mathrm{d}S_x \approx 0 \tag{35}$$

Combining with boundary conditions (20) and (21), one may find the rationality of approximations A1 and A2.

By using A1 and A2, Equation (30) will reduce to

$$u'_i(\mathbf{y}) \approx \int_\Omega (C_{mnk\ell}\bar{u}_{k,\ell n}(\mathbf{x}) + b_m(\mathbf{x}))G^{\infty}_{im}(\mathbf{y}-\mathbf{x})\,\mathrm{d}\Omega_x \tag{36}$$

After integration by parts, Equation (36) yields,

$$u'_i(\mathbf{y}) \approx \int_\Omega (C_{mnk\ell}\bar{u}_{k,\ell})G^{\infty}_{im,n}(\mathbf{y}-\mathbf{x})\,\mathrm{d}\Omega_x + \int_\Omega b_m G^{\infty}_{im}(\mathbf{y}-\mathbf{x})\,\mathrm{d}\Omega_x + \int_{\partial\Omega} \bar{\sigma}_{mn}(\mathbf{x})n_n G^{\infty}_{im}(\mathbf{y}-\mathbf{x})\,\mathrm{d}S_x \tag{37}$$

Consider the equilibrium equation in Ω,

$$\frac{\partial}{\partial x_n}\sigma_{mn} + b_m = 0 \Rightarrow \int_\Omega \left(\frac{\partial}{\partial x_n}\sigma_{mn} + b_m\right) G^\infty_{im}(\mathbf{y}-\mathbf{x})\,\mathrm{d}\Omega_x = 0$$

Integration by parts yields,

$$\int_{\partial\Omega} \sigma_{mn} n_n G^\infty_{im}(\mathbf{y}-\mathbf{x})\,\mathrm{d}S_x + \int_\Omega G^\infty_{im,n}(\mathbf{y}-\mathbf{x})\sigma_{mn}\,\mathrm{d}\Omega_x + \int_\Omega b_m G^\infty_{im}(\mathbf{y}-\mathbf{x})\,\mathrm{d}\Omega_x = 0 \tag{38}$$

Subtracting (38) from (37), we have

$$\begin{aligned} u'_i(\mathbf{y}) &\approx \int_\Omega (\bar{\sigma}_{mn}(\mathbf{x}) - \sigma_{mn}(\mathbf{x}))G^\infty_{im,n}(\mathbf{y}-\mathbf{x})\,\mathrm{d}\Omega_x \\ &\quad + \int_{\partial\Omega} (\bar{\sigma}_{mn}(\mathbf{x}) - \sigma_{mn}(\mathbf{x}))n_n G^\infty_{im}(\mathbf{y}-\mathbf{x})\,\mathrm{d}S_x \end{aligned} \tag{39}$$

Since $\sigma'_{mn} = \sigma_{mn} - \bar{\sigma}_{mn}$, the boundary integral in the above equation can be omitted due to the boundary condition (21) and the approximation A1. We then obtain the following estimate on the fine scale solution:

$$\begin{aligned} u'_i(\mathbf{y}) &\approx \int_\Omega (\bar{\sigma}_{mn}(\mathbf{x}) - \sigma_{mn}(\mathbf{x}))G^\infty_{im,n}(\mathbf{y}-\mathbf{x})\,\mathrm{d}\Omega_x \\ &= \int_\Omega C_{mnk\ell}(\bar{u}_{(k,\ell)}(\mathbf{x}) - u_{(k,\ell)}(\mathbf{x}))G^\infty_{im,n}(\mathbf{y}-\mathbf{x})\,\mathrm{d}\Omega_x \end{aligned} \tag{40}$$

Utilizing the symmetry conditions of the Green's function, we can express the fine scale strain in terms of the coarse scale strain, i.e.

$$\varepsilon'_{ij}(\mathbf{y}) \approx \frac{1}{4}\int_\Omega C_{mnk\ell}(G^\infty_{im,nj} + G^\infty_{jm,ni} + G^\infty_{in,mj} + G^\infty_{jn,mi})(\bar{u}_{(k,\ell)} - u_{(k,\ell)})\,\mathrm{d}\Omega_x \tag{41}$$

Now consider a planar subdivision of Ω, expressed as a set of elements $\{\Omega_e\}_{e\in\beta}$, $\beta = \{1, 2, \ldots, n_{el}\}$, where β is the index set of the subdivision and the number n_{el} is the total number of elements. Consider a spatial point $\mathbf{y}$ that belongs to Ω_e. We can express (41) as the sum of the integrals over each element:

$$\begin{aligned} \varepsilon'_{ij}(\mathbf{y}) &\approx \sum_{e\in\beta}\frac{1}{4}\int_{\Omega_e} C_{mnk\ell}(G^\infty_{im,nj} + G^\infty_{jm,ni} + G^\infty_{in,mj} + G^\infty_{jn,mi})(\bar{u}_{(k,\ell)} - u_{(k,\ell)})\,\mathrm{d}\Omega_x \\ &= \frac{1}{4}\int_{\Omega_I} C_{mnk\ell}(G^\infty_{im,nj} + G^\infty_{jm,ni} + G^\infty_{in,mj} + G^\infty_{jn,mi})(\bar{u}_{(k,\ell)} - u_{(k,\ell)})\,\mathrm{d}\Omega_x \\ &\quad + \sum_{e\in\beta\setminus\{I\}}\frac{1}{4}\int_{\Omega_e} C_{mnk\ell}(G^\infty_{im,nj}+G^\infty_{jm,ni}+G^\infty_{in,mj}+G^\infty_{jn,mi})(\bar{u}_{(k,\ell)}-u_{(k,\ell)})\,\mathrm{d}\Omega_x \end{aligned} \tag{42}$$

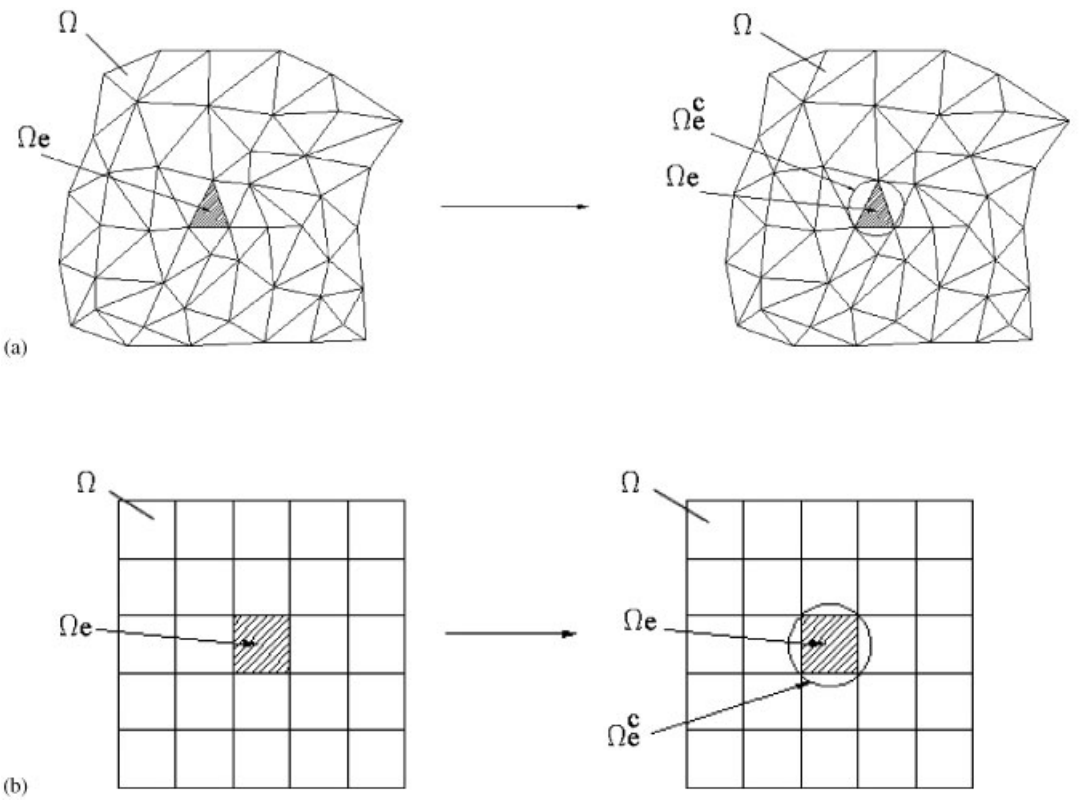

Figure 1. Illustration of the concept of equivalent element domain, Ω_e^c.

In order to evaluate the integrals, we now approximate the element domain Ω_e with an equivalent element domain Ω_e^c, which is the smallest circle that encloses the element Ω_e. In general, it is a hypersphere in $\mathbb{R}^d$. Figure 1 illustrates the selection of Ω_e^c.

Now we replace the element domain in the integrals of (42) with the equivalent element domain:

$$\varepsilon'_{ij}(\mathbf{y}) \approx \frac{1}{4}\int_{\Omega_I^c} C_{mnk\ell}(G^{\infty}_{im,nj} + G^{\infty}_{jm,ni} + G^{\infty}_{in,mj} + G^{\infty}_{jn,mi})(\bar{u}_{(k,\ell)} - u_{(k,\ell)})\,\mathrm{d}\Omega_x + \sum_{e\in\beta\setminus\{I\}} \frac{1}{4}\int_{\Omega_e^c} C_{mnk\ell}(G^{\infty}_{im,nj} + G^{\infty}_{jm,ni} + G^{\infty}_{in,mj} + G^{\infty}_{jn,mi})(\bar{u}_{(k,\ell)} - u_{(k,\ell)})\,\mathrm{d}\Omega_x \tag{43}$$

Referring to Appendix B, we can reduce the above equation to the following simpler form:

$$\varepsilon'_{ij}(\mathbf{y}) \approx \frac{1}{4}\int_{\Omega_I^c} C_{mnk\ell}(G^{\infty}_{im,nj} + G^{\infty}_{jm,ni} + G^{\infty}_{in,mj} + G^{\infty}_{jn,mi})\,\mathrm{d}\Omega_x \varepsilon^*_{k\ell}$$

$$+\sum_{e\in\beta\setminus\{I\}}\frac{1}{4}\int_{\Omega_e^c} C_{mnk\ell}(G^{\infty}_{im,nj}+G^{\infty}_{jm,ni}+G^{\infty}_{in,mj}+G^{\infty}_{jn,mi})\,\mathrm{d}\Omega_x\varepsilon^*_{k\ell} \tag{44}$$

Define tensors: $S^I_{ijk\ell}$ and $S^{Ee}_{ijk\ell}$:

$$S^I_{ijk\ell}(\mathbf{y}) := -\frac{1}{4}\int_{\Omega_e^c} C_{mnk\ell}(G^{\infty}_{im,nj}(\mathbf{y}-\mathbf{x})+G^{\infty}_{jm,ni}(\mathbf{y}-\mathbf{x}) +G^{\infty}_{in,mj}(\mathbf{y}-\mathbf{x})+G^{\infty}_{jn,mi}(\mathbf{y}-\mathbf{x}))\,\mathrm{d}\Omega_x \quad \forall \mathbf{y}\in\Omega_e^c \tag{45}$$

$$S^{Ee}_{ijk\ell}(\mathbf{y}) := -\frac{1}{4}\int_{\Omega\setminus\Omega_e^c} C_{mnk\ell}(G^{\infty}_{im,nj}(\mathbf{y}-\mathbf{x})+G^{\infty}_{jm,ni}(\mathbf{y}-\mathbf{x}) +G^{\infty}_{in,mj}(\mathbf{y}-\mathbf{x})+G^{\infty}_{jn,mi}(\mathbf{y}-\mathbf{x}))\,\mathrm{d}\Omega_x \quad \forall \mathbf{y}\notin\Omega_e^c \tag{46}$$

Then we can rewrite (44) in a compact form:

$$\varepsilon'_{ij}(\mathbf{y}) = S^I_{ijk\ell}(\mathbf{y})\varepsilon^*_{k\ell} + \sum_{e\in\beta\setminus\{I\}} S^{Ee}_{ijk\ell}(\mathbf{y})\varepsilon^*_{k\ell} \quad \text{for } \mathbf{y}\in\Omega_I \tag{47}$$

What we did in the above step is to separate the contribution to the fine scale strain into two parts: the interior part (the integral over Ω_I^c) and the exterior part (the integrals over Ω_e^c). The tensors $S^I_{ijk\ell}$ and $S^E_{ijk\ell}$ are the well-known Eshelby tensors [3, 4]. With our choice of Ω_e^c as a hypersphere, they both take explicit forms [18]:

$$S^I_{ijk\ell}(\bar{\mathbf{y}}) = \frac{1}{8(1-\nu)}((4\nu-1)\delta_{ij}\delta_{k\ell}+(3-4\nu)(\delta_{ik}\delta_{j\ell}+\delta_{i\ell}\delta_{jk})) \tag{48}$$

$$\begin{aligned} S^E_{ijk\ell}(\bar{\mathbf{y}}) = \frac{\rho^2}{8(1-\nu)}[&(\rho^2+4\nu-2)\delta_{ij}\delta_{k\ell}+(\rho^2-4\nu+2)(\delta_{ik}\delta_{j\ell}+\delta_{i\ell}\delta_{jk})\\ &+4(1-\rho^2)\delta_{ij}r_kr_\ell+4(1-2\nu-\rho^2)\delta_{k\ell}r_ir_j\\ &+4(\nu-\rho^2)(\delta_{ik}r_jr_\ell+\delta_{jk}r_ir_\ell+\delta_{i\ell}r_jr_k+\delta_{j\ell}r_ir_k)+8(3\rho^2-2)r_ir_jr_kr_\ell] \end{aligned} \tag{49}$$

The $\bar{\mathbf{y}}$ in the above equations is the local co-ordinate: each Ω_e^c has a local co-ordinate system with an origin at the centre of the hypersphere (shown in Figure 2). If we denote the centre of Ω_e^c as $\mathbf{y}_c^e$, then $\bar{\mathbf{y}} = \mathbf{y}-\mathbf{y}_c^e$. Also in the above equations, $r_i = \bar{y}_i/|\bar{\mathbf{y}}|$ and $\rho = a/|\bar{\mathbf{y}}|$ with a the radius of Ω_e^c. The expressions of S^I_{ijkl} and S^E_{ijkl} for plane stress problems can be obtained by replacing ν in the above equations by

$$\nu' = \frac{\nu}{1+\nu} \tag{50}$$

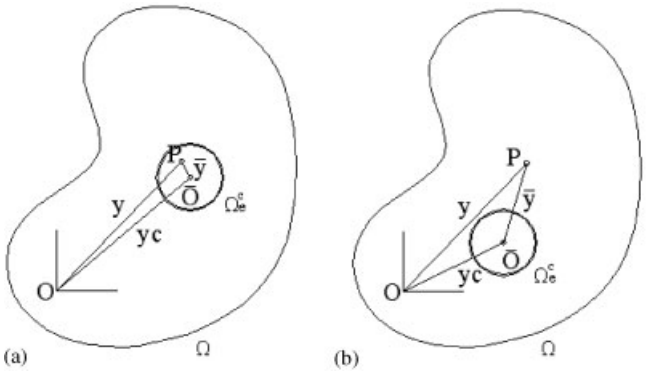

Figure 2. The local co-ordinate system for the subdomain Ω_e^c: (a) interior case; and (b) exterior case.

A detailed derivation of the 2D interior Eshelby tensor, $S^I_{ijk\ell}$ can be found in Appendix A. Examining the expressions of the Eshelby tensors, we find that $S^I_{ijk\ell}$ is a constant tensor, whereas $S^E_{ijk\ell}$ is of order $\mathcal{O}(\rho^2)$ and $\rho < 1$ for $\mathbf{y} \notin \Omega_e^c$. This clearly shows that the exterior contribution is a second-order contribution that is much smaller than the interior contribution and decays fast when $\mathbf{y}$ is away from Ω_e^c. Based on this fact, we make a further approximation by neglecting the exterior parts of the fine scale strain, which represents the interaction of discretization error among different elements

A3. The exterior parts of the fine scale solution can be neglected, since they are of order $\mathcal{O}(\rho^2)$.

That leads to the expression:

$$\varepsilon'_{ij}(\mathbf{y}) = S^I_{ijk\ell}\varepsilon^*_{k\ell} \quad \text{for } \mathbf{y} \in \Omega_I \tag{51}$$

Since no exterior Eshelby tensor is present in the fine scale solution, we replace $S^I_{ijk\ell}$ with $S_{ijk\ell}$ without causing any confusion. Finally, $\forall \mathbf{y} \in \Omega$, we have the fine scale strain solution

$$\varepsilon'_{ij}(\mathbf{y}) = \sum_{e=1}^{n_{el}} \{S_{ijk\ell}(u_{(k,\ell)} - \bar{u}^e_{(k,\ell)})\chi(\Omega_e)\} \tag{52}$$

where $\chi(\Omega_e)$ is the characteristic function of the element Ω_e,

$$\chi(\Omega_e) = \begin{cases} 1, & \mathbf{y} \in \Omega_e \\ 0, & \mathbf{y} \in \Omega/\Omega_e \end{cases} \tag{53}$$

Remark 3.1
By neglecting the exterior parts of the fine scale strain expression, we actually neglect the interaction of discretization error between elements. Our justification for doing so is by showing that each exterior part is of second order smaller than the interior part.

Our previous derivation starts from (29), which is a global expression. Another way of calculating the fine scale strain is to start from a local formulation: using Ω_e^c instead of the

whole Ω as the integral domain:

$$u'_i(\mathbf{y}) = \int_{\Omega_e^c} (C_{mnk\ell}\bar{u}_{k,\ell n} + b_m) G_{im}^{\infty}(\mathbf{y}-\mathbf{x})\,\mathrm{d}\Omega_x + \int_{\partial\Omega_e^c} \sigma'_{mn}(\mathbf{x}) n_n G_{im}^{\infty}(\mathbf{y}-\mathbf{x})\,\mathrm{d}S_x + \int_{\partial\Omega_e^c} \sigma_{k\ell}^{G_i^{\infty}}(\mathbf{y}-\mathbf{x}) n_\ell u'_k(\mathbf{x})\,\mathrm{d}S_x \tag{54}$$

for $\mathbf{y} \in \Omega_e^c$. If we make approximations to neglect the fine scale solution on $\partial\Omega_e^c$, i.e.

B1.

$$\int_{\partial\Omega_e^c} \sigma'_{ij} n_j G_{im}^{\infty}\,\mathrm{d}S_x \approx 0 \tag{55}$$

B2.

$$\int_{\partial\Omega_e^c} \sigma_{k\ell}^{G_m^{\infty}}(\mathbf{y}-\mathbf{x}) n_\ell u'_k(\mathbf{x})\,\mathrm{d}S_x \approx 0 \tag{56}$$

Then (54) will reduce to

$$u'_i(\mathbf{y}) = \int_{\Omega_e^c} (C_{mnk\ell}\bar{u}_{k,\ell n}(\mathbf{x}) + b_m(\mathbf{x})) G_{im}^{\infty}(\mathbf{y}-\mathbf{x})\,\mathrm{d}\Omega_x \tag{57}$$

If we go through the similar procedures as the previous, it is not difficult to show that we will end up with the same final fine scale strain solution (52). This shows that the approximations B1 and B2 are equivalent to the approximations we made in the global formulation, i.e. approximations A1, A2 and the omittance of the exterior parts.

We acknowledge the fact that the approximations that we made down the stretch made our derivation less stringent. The similar approximations, however, have also been used in almost all the other variational multiscale formulations. For example, in his original papers [12, 14]. Hughes also neglect the fine scale interaction among different elements, which is equivalent to the approximation A3 in this paper. In this part of the work, we are content to live with these approximations. A better formulation to eliminate some of approximations made above will be presented in Part II of this work. For instance, to eliminate use of B1 and B2, one can use Green's function for a finite domain. Then the Green's function G_{im} and the resulted traction will vanish on the local boundaries, and thus the approximations B1 and B2, or equivalently A1–A3, may be rigorously justified.

3.2. A smart element based on the Zienkiewicz–Zhu estimate

To this end, we still cannot calculate the element eigenstrain,

$$\varepsilon_{ij}^{*}(\mathbf{x}) = (u_{(i,j)} - \bar{u}_{(i,j)}) \quad \forall \mathbf{x} \in \Omega_e \tag{58}$$

because in general we do not know the exact solution.

To find the element eigenstrain, the Zienkiewicz–Zhu criterion is used to estimate the discretization error of coarse scale and it is used to self-adaptively adjust the coarse scale stiffness matrix.

The departure point of this smart element is the fine scale representation (40). Neglecting interaction among elements, we may write

$$u'_i(\mathbf{y}) = \int_{\Omega_e} C_{mnk\ell}(\bar{u}^e_{(k,\ell)}(\mathbf{x}) - u_{(k,\ell)}(\mathbf{x}))G^{\infty}_{im,n}(\mathbf{y}-\mathbf{x})\,\mathrm{d}\Omega_x \tag{59}$$

Intuitively, the element eigenstrain, $u_{(k,\ell)} - \bar{u}^e_{(k,\ell)}$, in Equation (59) represents *a priori* error estimate of coarse scale solution. Nevertheless, it is impossible to solve Equation (52) because we do not know the exact solution $u_{(k,\ell)}$. We need to replace the *a priori eigenstrain* with *a posteriori eigenstrain*, in order to introduce a feedback mechanism to correct or to 'control' the numerical pollution in coarse scale finite element computation. To do so, we choose the popular Zienkiewicz–Zhu's *a posteriori estimate* as the feedback signal.

The essence of the Zienkiewicz–Zhu estimate is to use a smoothing technique to find a recovered displacement gradient field that is more accurate than the coarse scale displacement gradient field, which can then provide at least the first-order error estimate for the coarse scale solution. Denote the Zienkiewicz–Zhu recovery displacement gradient field as $u^Z_{(k,\ell)}$ and replace the exact displacement gradient, $u_{(k,\ell)}$, with the recovered solution, $u^Z_{(k,\ell)}$. We can then find the *a posteriori* eigenstrain,

$$\varepsilon^*_{k\ell} = u^Z_{(k,\ell)} - \bar{u}_{(k,\ell)} \tag{60}$$

Subsequently, we have the following fine scale correction:

$$u'_i(\mathbf{y}) = \int_{\Omega_e} C_{mnk\ell}(\bar{u}^e_{(k,\ell)}(\mathbf{x}) - u^Z_{(k,\ell)}(\mathbf{x}))G^{\infty}_{im,n}(\mathbf{y}-\mathbf{x})\,\mathrm{d}\Omega_x \quad \mathbf{y}\in\Omega_e \tag{61}$$

Hence Equation (52) becomes,

$$\varepsilon'_{ij}(\mathbf{x}) \approx S_{ijk\ell}(u^Z_{(k,\ell)}(\mathbf{x}) - \bar{u}^e_{(k,\ell)}(\mathbf{x})) \qquad \forall \mathbf{x}\in\Omega_e \tag{62}$$

To find the recovery displacement gradient in an element, $u^Z_{(k,\ell)}, \forall \mathbf{x}\in\Omega_e$, we follow the procedure outlined in References [10, 11]. $u^Z_{(k,\ell)}$ is defined by the basis functions N^n, the same basis functions as the ones used for the interpolation of displacements, and the nodal parameters $\tilde{u}^{Z,n}_{(k,\ell)}$. Superscript n is used here to denote a particular node. The recovered displacement gradient field can be written as

$$u^Z_{(k,\ell)}(\mathbf{x}) = \sum_{n=1}^{n_{ed}} N^n(\mathbf{x})\tilde{u}^{Z,n}_{(k,\ell)} \tag{63}$$

It is assumed that the nodal values belong to a polynomial expansion of the same order as that in the basis function of the displacement, which is valid over the element cluster surrounding the node under consideration.

$$\tilde{u}^{Zp}_{(k,\ell)}(\mathbf{x}) = \mathbf{P}(\mathbf{x})\mathbf{a}^{\mathbf{n}}_{(\mathbf{k},\ell)} \tag{64}$$

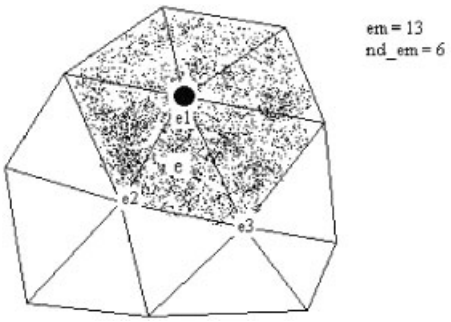

Figure 3. Nodal patch and element cluster assembly.

The unknown parameters $\mathbf{a}^n$ are obtained by minimizing the *a posteriori* eigenstrain in a nodal patch with total element number *em*, (see Figure 3). $\mathbf{P}(\mathbf{x})$ is a monomial basis. For a triangle element mesh, we may choose $\mathbf{P}(\mathbf{x}) = [1, x, y]$, and for a quadrilateral element mesh, we choose $\mathbf{P}(\mathbf{x}) = [1, x, y, xy]$.

The nodal values are then obtained by substituting appropriate co-ordinates of the node into the polynomial expansion,

$$\tilde{u}^{Z,n}_{(k,\ell)}(\mathbf{x}) = \mathbf{P^n}(\mathbf{x})\mathbf{a^n_{(k,\ell)}} \tag{65}$$

where $\mathbf{P^n}(\mathbf{x})$ is the monomial basis for the node n. $\mathbf{a^n_{(k,\ell)}}$ is the vector obtained at node n for the (k, ℓ) component of the strain.

The unknown vector $\mathbf{a^n_{(k,\ell)}}$ is determined by the minimization condition of $E(\mathbf{a^n_{(k,\ell)}})$

$$\begin{aligned} E(\mathbf{a^n_{(k,\ell)}}) &= \int_{\Omega_E} (\tilde{u}^{Zp}_{(k,l)} - \bar{u}_{(k,l)})^2 \, \mathrm{d}\Omega = \int_{\Omega_E} (\mathbf{P}\mathbf{a^n_{(k,\ell)}} - \bar{u}_{(k,l)})^2 \, \mathrm{d}\Omega \\ &= \sum_{e_j=1}^{em} \int_{\Omega_{e_j}} (\mathbf{P}_{e_j}\mathbf{a^n_{(k,\ell)}} - \bar{u}^{e_j}_{(k,l)})^2 \, \mathrm{d}\Omega \end{aligned} \tag{66}$$

where $\Omega_E = \bigcup_{e_j=1}^{em} \Omega_{e_j}$ is an element cluster surrounding the node under consideration.

$$\left(\int_{\Omega_E} \mathbf{P}^{\mathrm{T}}\mathbf{P} \, \mathrm{d}\Omega \right) \mathbf{a^n_{(k,\ell)}} = \int_{\Omega_E} \mathbf{P}^{\mathrm{T}} \bar{u}_{(k,l)} \, \mathrm{d}\Omega \tag{67}$$

In the matrix form, this can be written as

$$u^{Zp}_{(k,l)} = \mathbf{P}\mathbf{a^n_{(k,\ell)}} = \mathbf{P}\mathbf{A}^{n^{-1}}\mathbf{b^n_{(k,\ell)}} \tag{68}$$

where

$$\mathbf{A}^{n^{-1}} = \int_{\Omega_E} \mathbf{P}^{\mathrm{T}}\mathbf{P} \, \mathrm{d}\Omega \quad \text{and} \quad \mathbf{b^n_{(k,\ell)}} = \int_{\Omega_E} \mathbf{P}^{\mathrm{T}} \bar{u}_{(k,l)} \, \mathrm{d}\Omega \tag{69}$$

For a 2D triangle element, the coarse scale displacement gradient field is piecewise constant, therefore,

$$\tilde{u}^{Z,n}_{(k,l)} = \mathbf{P}^n \mathbf{A}^{n^{-1}} \left[\sum_{e_j=1}^{em} \left(\int_{\Omega_{e_j}} \mathbf{P}^{\mathrm{T}}_{e_j} \, \mathrm{d}\Omega \right) \bar{u}^{e_j}_{(k,l)} \chi(\Omega_{e_j}) \right] \tag{70}$$

The fine scale correction due to the element, e, is

$$\varepsilon'_{ij}(\mathbf{x}) = S_{ijk\ell} \left\{ \sum_{n=1}^{n_{ed}} N^n(\mathbf{x}) \mathbf{P}^n \mathbf{A}^{n^{-1}} \left[\sum_{e_j=1}^{em} \left(\int_{\Omega_{e_j}} \mathbf{P}^{\mathrm{T}}_{e_j} \, \mathrm{d}\Omega \right) \bar{u}^{e_j}_{(k,\ell)} \chi(\Omega_{e_j}) \right] - \bar{u}^{e}_{(k,\ell)} \chi(\Omega_e) \right\} \quad \forall \mathbf{x} \in \Omega_e \tag{71}$$

In general,

$$\varepsilon'_{ij}(\mathbf{x}) = S_{ijk\ell} \left\{ \sum_{n=1}^{n_{ed}} N^n(\mathbf{x}) \mathbf{P}^n \mathbf{A}^{n^{-1}} \left[\sum_{e_j=1}^{em} \left(\int_{\Omega_{e_j}} \mathbf{P}^{\mathrm{T}}_{e_j} \bar{u}^{e_j}_{(k,\ell)} \, \mathrm{d}\Omega \right) \right] - \bar{u}^{e}_{(k,\ell)}(\mathbf{x}) \chi(\Omega_e) \right\} \quad \forall \mathbf{x} \in \Omega_e \tag{72}$$

One may observe the non-local nature of the Zienkiewicz–Zhu recovery solution.

4. FINITE ELEMENT IMPLEMENTATION

We now discuss the finite element implementation. Consider the coarse scale weak formulation,

$$a(\bar{\mathbf{w}}, \bar{\mathbf{u}}) + a(\bar{\mathbf{w}}, \mathbf{u}') = (\bar{\mathbf{w}}, \mathbf{f})_\Omega + (\bar{\mathbf{w}}, \mathbf{t}^0)_{\Gamma_t} \tag{73}$$

Substituting (72) into (73), we have

$$\begin{aligned} a(\bar{\mathbf{w}}, \bar{\mathbf{u}}) + a(\bar{\mathbf{w}}, \mathbf{u}') &= \int_\Omega \bar{w}_{(i,j)} C_{ijk\ell} \left\{ \bar{u}_{(k,\ell)} + S_{k\ell mn} \left[\sum_{n=1}^{n_{ed}} N^n(\mathbf{x}) \mathbf{P}^n \mathbf{A}^{n^{-1}} \right.\right. \\ &\quad \left.\left. \times \left(\sum_{e_j=1}^{em} \left(\int_{\Omega_{e_j}} \mathbf{P}^{\mathrm{T}}_{e_j} \bar{u}^{e_j}_{(m,n)} \, \mathrm{d}\Omega_x \right) \right) - \bar{u}^{e}_{(m,n)}(\mathbf{x}) \chi(\Omega_e) \right] \right\} \mathrm{d}\Omega_x \\ &= (\bar{\mathbf{w}}, \mathbf{b})_\Omega + (\bar{\mathbf{w}}, \mathbf{t}^0)_{\Gamma_t} \\ &= \int_\Omega \bar{w}_i b_i \, \mathrm{d}\Omega_x + \int_{\Gamma_t} \bar{w}_i t^0_i \, \mathrm{d}S_x \end{aligned} \tag{74}$$

Equation (74) can then be rewritten as

$$\mathop{\boldsymbol{A}}_{e=1}^{n_{el}} \int_{\Omega_e} \bar{w}^e_{(i,j)} C_{ijkl} \left\{ \bar{u}^e_{(k,\ell)} + S_{k\ell mn} \left[\sum_{n=1}^{n_{ed}} N^n(\mathbf{x}) \mathbf{P}^n \mathbf{A}^{n-1} \left(\sum_{e_j=1}^{em} \left(\int_{\Omega_{e_j}} \mathbf{P}^{\mathrm{T}}_{e_j} \bar{u}^{e_j}_{(m,n)} \, \mathrm{d}\Omega_x \right) \right) \right. \right.$$

$$\left. \left. - \bar{u}^e_{(m,n)}(\mathbf{x}) \right] \right\} \mathrm{d}\Omega_x = \mathop{\boldsymbol{A}}_{e=1}^{n_{el}} \left\{ \int_{\Omega_e} \bar{w}^e_i b_i \, \mathrm{d}\Omega_x + \int_{\Gamma_t \cap \partial\Omega_e} \bar{w}^e_i t^0_i \, \mathrm{d}S_x \right\} \tag{75}$$

Consider the FEM discretization. We can write (75) in a matrix form

$$[\mathbf{K}][\mathbf{d}] = [\mathbf{R}] \tag{76}$$

The self-adaptive stiffness matrix based on the Zienkiewicz–Zhu feedback is

$$\mathbf{K} = \mathop{\boldsymbol{A}}_{e=1}^{n_{el}} \int_{\Omega_e} [\mathbf{B}]^{\mathrm{T}}_e [\mathbf{C}] \left\{ [\mathbf{B}]_e + [\mathbf{S}] \left[\sum_{n=1}^{n_{ed}} N^n(\mathbf{x}) [\mathbf{P}^n] [\mathbf{A}^{n-1}] \left(\sum_{e_j=1}^{em} [\mathbf{b}^n_{e_j}] \right) - [\mathbf{B}]_e \right] \right\} \mathrm{d}\Omega_x \tag{77}$$

where

$$[\mathbf{P}^n] = \begin{bmatrix} \mathbf{P}^n & \mathbf{0} & \mathbf{0} \\ \mathbf{0} & \mathbf{P}^n & \mathbf{0} \\ \mathbf{0} & \mathbf{0} & \mathbf{P}^n \end{bmatrix} \tag{78}$$

$$[\mathbf{A}^{n-1}] = \begin{bmatrix} \mathbf{A}^{n-1} & \mathbf{0} & \mathbf{0} \\ \mathbf{0} & \mathbf{A}^{n-1} & \mathbf{0} \\ \mathbf{0} & \mathbf{0} & \mathbf{A}^{n-1} \end{bmatrix} \tag{79}$$

and

$$[\mathbf{b}^n_{e_j}] = \begin{bmatrix} \displaystyle\int_{\Omega_{e_j}} \mathbf{P}^{\mathrm{T}}_{e_j} (1^1)^{\mathrm{T}} [\mathbf{B}]_{e_j} \, \mathrm{d}\Omega_x \\ \displaystyle\int_{\Omega_{e_j}} \mathbf{P}^{\mathrm{T}}_{e_j} (1^2)^{\mathrm{T}} [\mathbf{B}]_{e_j} \, \mathrm{d}\Omega_x \\ \displaystyle\int_{\Omega_{e_j}} \mathbf{P}^{\mathrm{T}}_{e_j} (1^3)^{\mathrm{T}} [\mathbf{B}]_{e_j} \, \mathrm{d}\Omega_x \end{bmatrix} \tag{80}$$

where $(1^1)^{\mathrm{T}} = [1, 0, 0]$ etc. The global force vector $[\mathbf{R}]$ is

$$[\mathbf{R}] = \mathop{\boldsymbol{A}}_{e=1}^{n_{el}} \left\{ \int_{\Omega_e} [\mathbf{N}]_e [\mathbf{b}]_e \, \mathrm{d}\Omega_x + \int_{\Omega_e \cap \Gamma_t} [\mathbf{N}]_e [\mathbf{t}^0]_e \, \mathrm{d}S_x \right\} \tag{81}$$

where the symbol $\boldsymbol{A}$ is the so-called *element assembly operator* (see Reference [20]) and $[\mathbf{N}]_e$ and $[\mathbf{B}]_e$ are the element shape function matrix and shape function gradient matrix, respectively.

$[\mathbf{b}]_e$ is the element body force vector and $[\mathbf{t}^0]_e$ is the element traction vector. $[\mathbf{C}]$ and $[\mathbf{S}]$ are the matrix form of the elasticity tensor and the Eshelby's tensor. For plane strain case, they are:

$$[\mathbf{C}] = \begin{bmatrix} \lambda + 2G & \lambda & 0 \\ \lambda & \lambda + 2G & 0 \\ 0 & 0 & G \end{bmatrix}, \quad \lambda = \frac{vE}{(1+v)(1-2v)} \quad \text{and} \quad G = \frac{E}{2(1+v)} \tag{82}$$

$$[\mathbf{S}] = \frac{1}{8(1-v)} \begin{bmatrix} 5-4v & 4v-1 & 0 \\ 4v-1 & 5-4v & 0 \\ 0 & 0 & 3-4v \end{bmatrix} \tag{83}$$

Remark 4.1

Consider an element cluster with total elements, $em = 13$, the number of elements adjacent to the node n_d, $nd_{em} = 6$, and number n_{ed} is the number of nodes in an element. In Equation (77), there are two assembly operators: inside assembly operator and outside assembly operator. For constant strain triangle elements, the element patch assembly operation can be understood as

$$[\mathbf{A}]_e^{-1} \left(\mathop{\boldsymbol{A}}_{e_j=1}^{em} \int_{\Omega_{e_j}} [\mathbf{P}]_{e_j}^{\mathrm{T}} \, \mathrm{d}\Omega_x \right) = \begin{bmatrix} \alpha_{11} & \alpha_{12} & \cdots & \alpha_{1em} \\ \alpha_{21} & \ddots & & \vdots \\ \vdots & & \ddots & \vdots \\ \alpha_{2n_{ed}1} & \cdots & \cdots & \alpha_{2n_{ed}em} \end{bmatrix}^{2n_{ed} \times em} \tag{84}$$

where α_{ij} are constants such that

$$\sum_{j=1}^{em} \alpha_{e_i j} = 1, \quad e_i = 1, 2, \ldots, 2n_{ed} \tag{85}$$

In fact, in each row, e_i, there are only nd_{em} numbers of $\alpha_{e_i j}$'s that are non-zero, and they are the weights of strains, $\bar{u}_{(i,j)}$, contributed from the elements adjacent to the element, e, and sharing the node, e_I. Note that each row e_i corresponds to a degree of freedom, and in each element there are $2n_{ed}$ of degrees of freedom. We denote a nodal point in an element as e_I, see Figure 3.

5. NUMERICAL EXAMPLES

To validate the proposed smart element method, two numerical examples have been carried out. In each problem, both conventional FEM method and the smart element method are used. We then compare the numerical results.

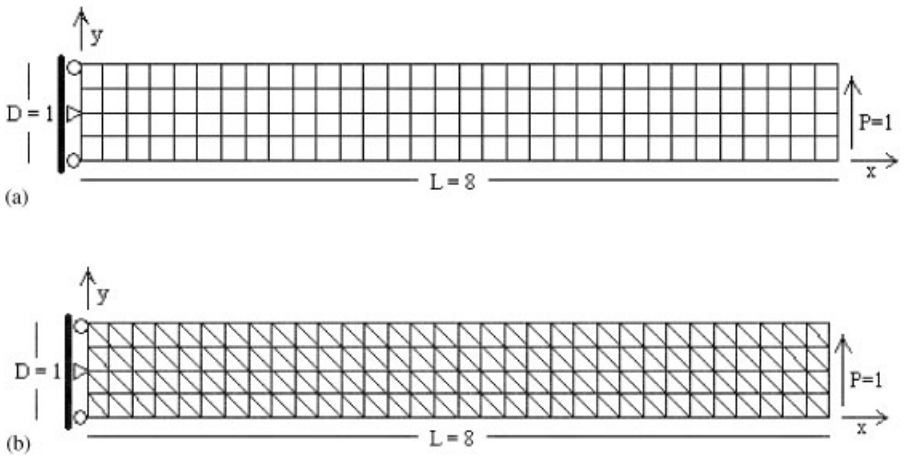

Figure 4. A cantilever beam with: (a) quadrilateral mesh; and (b) triangle mesh.

5.1. Cantilever beam

We try to solve the bending problem of a cantilever beam subjected to end loading (Figure 4). The exact solution of this problem is given by Timoshenko and Goodier [21],

$$u_x = -\frac{Py}{6\bar{E}I}\left(y - \frac{D}{2}\right)[3x(2L - x) + (2 + \bar{\nu})y(y - D)] \tag{86}$$

$$u_y = \frac{P}{6\bar{E}I}\left[x^2(3L - x) + 3\bar{\nu}(L - x)\left(y - \frac{D}{2}\right)^2 + \frac{4 + 5\bar{\nu}}{4}D^2x\right] \tag{87}$$

where

$$I = \frac{D^3}{12} \tag{88}$$

$$\bar{E} = \begin{cases} E & \text{for plane stress} \\ E/(1 - \nu^2) & \text{for plane strain} \end{cases} \tag{89}$$

$$\bar{\nu} = \begin{cases} \nu & \text{for plane stress} \\ \nu/(1 - \nu) & \text{for plane strain} \end{cases} \tag{90}$$

The corresponding stress field is

$$\sigma_{xx}(x, y) = -\frac{P}{I}(L - x)\left(y - \frac{D}{2}\right) \tag{91}$$

$$\sigma_{yy}(x, y) = 0 \tag{92}$$

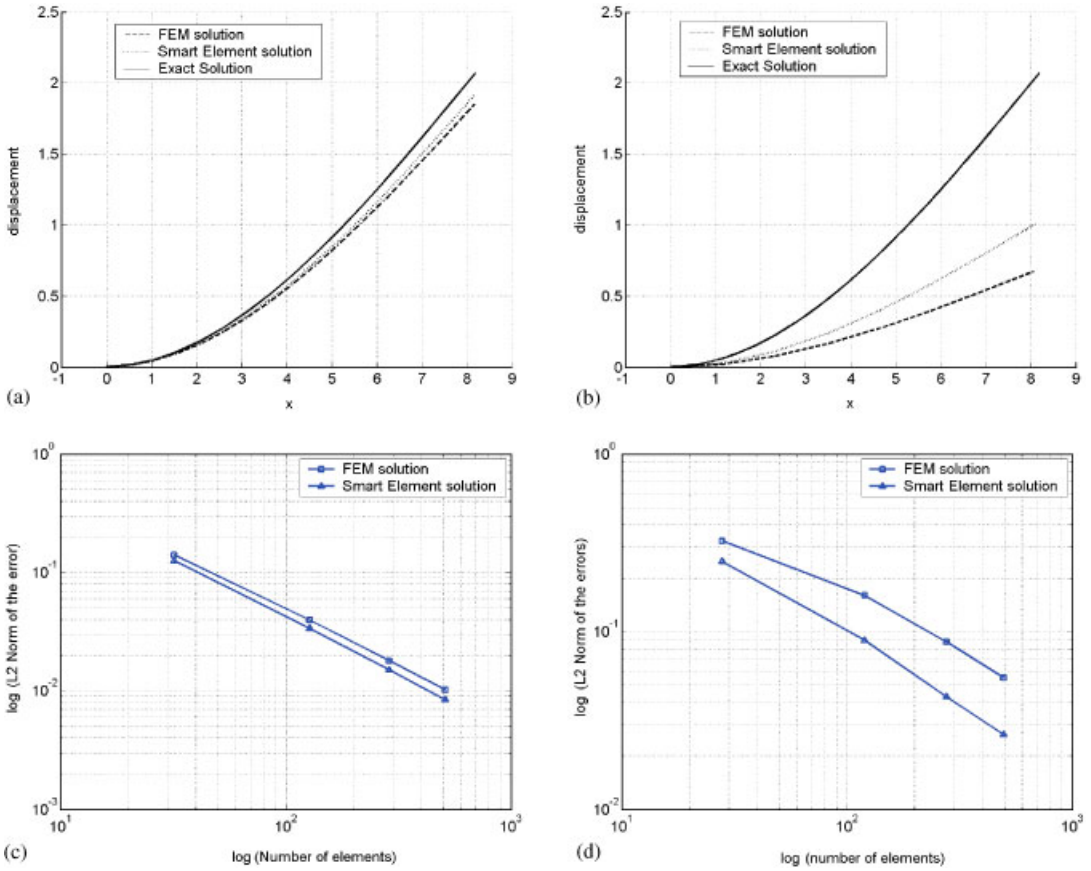

Figure 5. Comparison of smart element method results to conventional FEM solution and the exact solution: (a) displacement contour of the $y = 0$ edge, quadrilateral element; (b) displacement contour of the $y = 0$ edge, triangle element; (c) log–log convergence plot in term of the L_2 norm of the error, quadrilateral element; and (d) log–log convergence plot in term of the L_2 norm of the error, triangle element.

$$\sigma_{xy}(x, y) = \frac{Py}{2I}(y - D) \tag{93}$$

The problem has been solved for the plane strain case with Young's modulus $E = 1000$, Poisson's ratio $v = 0.25$, and zero body force, i.e. $b_m = 0.0$. The dimensions of the beam are: $L = 8.0$ and $D = 1.0$. The prescribed traction and prescribed displacement boundary conditions are illustrated in Figure 4, where Figure 4(a) shows the quadrilateral mesh and (b) shows the triangular mesh. Displacement boundary conditions are imposed along the boundary $x = 0$ by using the exact solution (86) and (87). The applied traction is imposed on the boundary $x = L$. The rest of the boundary is traction free.

The numerical results obtained via smart element method are compared to both the exact solution and the conventional finite element solution in Figure 5. From Figures 5(a) and (b),

we can see that the smart element solution shows point-wise improvement over the conventional FEM solution. Figures 5(c) and (d) show the convergence of the smart element method with increasing number of elements. They also show that the smart element method is more accurate than the conventional FEM in term of the overall error L_2 norm, which is defined as (e.g. Reference [22])

$$\eta_{L_2} = \frac{\|\mathbf{e}\|_{L_2}}{\|\mathbf{u}\|_{L_2}} \tag{94}$$

where

$$\|\mathbf{e}\|_{L_2} = \left[\int_\Omega (\mathbf{u} - \mathbf{u}^h)^{\mathrm{T}}(\mathbf{u} - \mathbf{u}^h)\,\mathrm{d}\Omega\right]^{\frac{1}{2}} \tag{95}$$

$$\|\mathbf{u}\|_{L_2} = \left[\int_\Omega \mathbf{u}^{\mathrm{T}}\mathbf{u}\,\mathrm{d}\Omega\right]^{\frac{1}{2}} \tag{96}$$

with $\mathbf{u}$ the exact solution and $\mathbf{u}^h$ the numerical solution.

5.2. A plate with a hole

In this section, we study the problem of a finite square plate with a hole at the centre, subjected to an unit uniaxial tension along x-direction (Figure 6(a)). The exact solution of this problem is given as

$$u_1(r,\theta) = \frac{a}{8\mu}\left[\frac{r}{a}(\kappa+1)\cos\theta + 2\frac{a}{r}((1+\kappa)\cos\theta + \cos 3\theta) - 2\frac{a^3}{r^3}\cos 3\theta\right] \tag{97}$$

$$u_2(r,\theta) = \frac{a}{8\mu}\left[\frac{r}{a}(\kappa-3)\sin\theta + 2\frac{a}{r}((1-\kappa)\sin\theta + \sin 3\theta) - 2\frac{a^3}{r^3}\sin 3\theta\right] \tag{98}$$

where μ is the shear modulus and κ (Kolosov constant) is defined as

$$\kappa = \begin{cases} 3 - 4\nu & \text{for plane strain} \\ \dfrac{3-\nu}{1+\nu} & \text{for plane stress} \end{cases} \tag{99}$$

The corresponding stress field is

$$\sigma_{11}(r,\theta) = 1 - \frac{a^2}{r^2}\left(\frac{3}{2}\cos 2\theta + \cos 4\theta\right) + \frac{3}{2}\frac{a^4}{r^4}\cos 4\theta \tag{100}$$

$$\sigma_{22}(r,\theta) = -\frac{a^2}{r^2}\left(\frac{1}{2}\cos 2\theta - \cos 4\theta\right) - \frac{3}{2}\frac{a^4}{r^4}\cos 4\theta \tag{101}$$

$$\sigma_{12}(r,\theta) = -\frac{a^2}{r^2}\left(\frac{1}{2}\sin 2\theta + \sin 4\theta\right) + \frac{3}{2}\frac{a^4}{r^4}\sin 4\theta \tag{102}$$

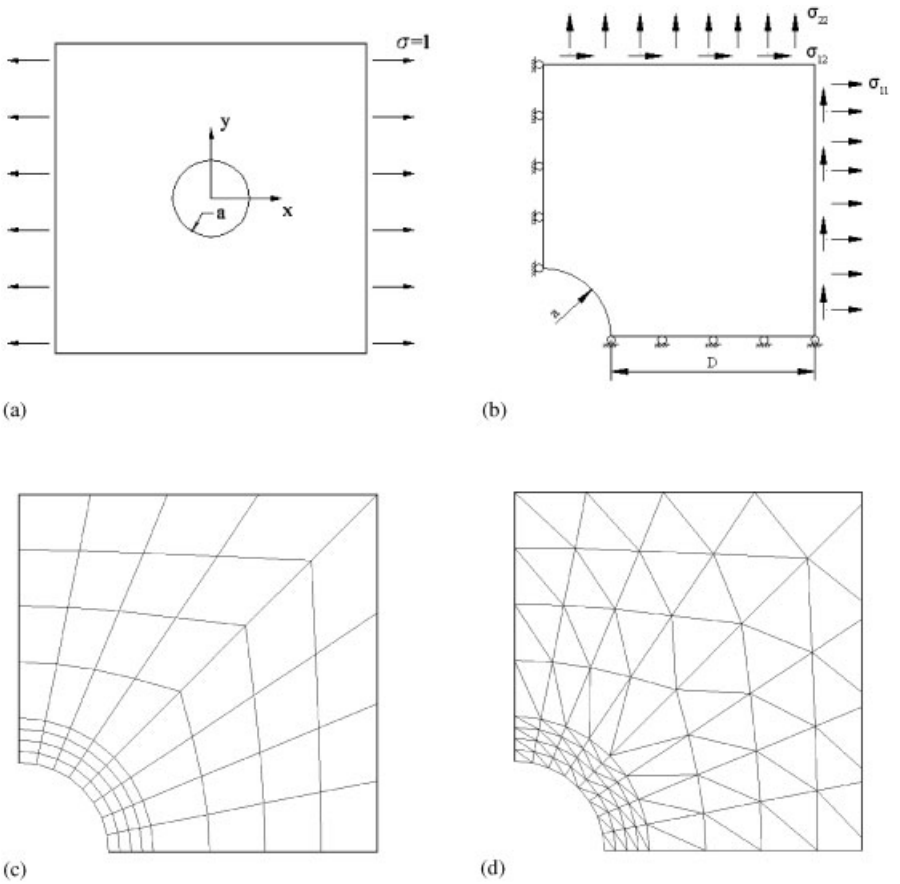

Figure 6. A plate with a hole: (a) problem setting; (b) actual model with boundary conditions; (c) a sample quadrilateral mesh; and (d) a sample triangular mesh.

We solve the problem for the plane strain case with Young's modulus $E = 1$, Poisson's ratio $v = 0.25$, and zero body force, i.e. $b_m = 0.0$. Due to symmetry only one quadrant of the plate is considered for the analysis. The dimensions of one quarter of the plate and prescribed traction/displacement boundary conditions are illustrated in Figure 6(b). Note that the traction boundary condition is imposed along $x = (a + D)$ and $y = (a + D)$ by using the exact solution (100)–(102). The rest of the boundary is traction free. Figure 6 shows the two sample meshes used in computations.

Figure 7 shows the deformed meshes computed by the smart element method, the conventional FEM and the exact solution. We can see the point-wise improvement of the smart element method solution. Figure 8 illustrates the same point by plotting error norms of each element, comparing the smart element solution to the conventional FEM solution. Both error L_2 norm and error energy norm are plotted, with the later defined as

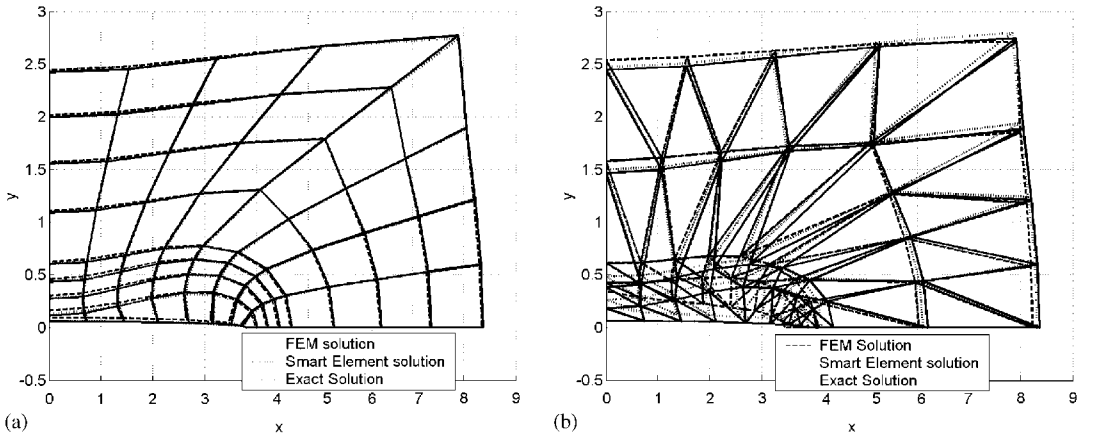

Figure 7. Smart element solution shows point-wise improvement: (a) the deformed meshes, quadrilateral element; and (b) the deformed meshes, triangle element.

(e.g. Reference [22]):

$$\eta = \frac{\|\mathbf{e}\|}{\|\mathbf{u}\|} \tag{103}$$

where

$$\|\mathbf{e}\| = \left[\int_{\Omega} (\boldsymbol{\sigma} - \boldsymbol{\sigma}^h)^{\mathrm{T}} \mathbf{C}^{-1} (\boldsymbol{\sigma} - \boldsymbol{\sigma}^h)\, \mathrm{d}\Omega\right]^{\frac{1}{2}} \tag{104}$$

$$\|\mathbf{u}\| = \left[\int_{\Omega} \boldsymbol{\sigma}^{\mathrm{T}} \mathbf{C}^{-1} \boldsymbol{\sigma}\, \mathrm{d}\Omega\right]^{\frac{1}{2}} \tag{105}$$

The stress is used to compute energy norm since we know the exact stress solution. We note that the smart element solution shows improvement in both the error L_2 norm and the error energy norm.

The convergence result is shown in Figure 9. Again we can see smart element method provides more accurate result than conventional FEM, i.e. its convergence path is always below the FEM convergence path, and it is convergent to the exact solution.

5.3. The nearly incompressible material test

We used the smart element formulation to calculate the plate with a hole problem under the nearly incompressible condition ($v \to 0.5$). It is well known that the incompressibility will lead to volumetric locking in conventional FEM solution. We are interested in examining the performance of the smart element method under such condition. We carry out the calculation using the same problem as in the last example, adopting $v = 0.49$ and 0.499.

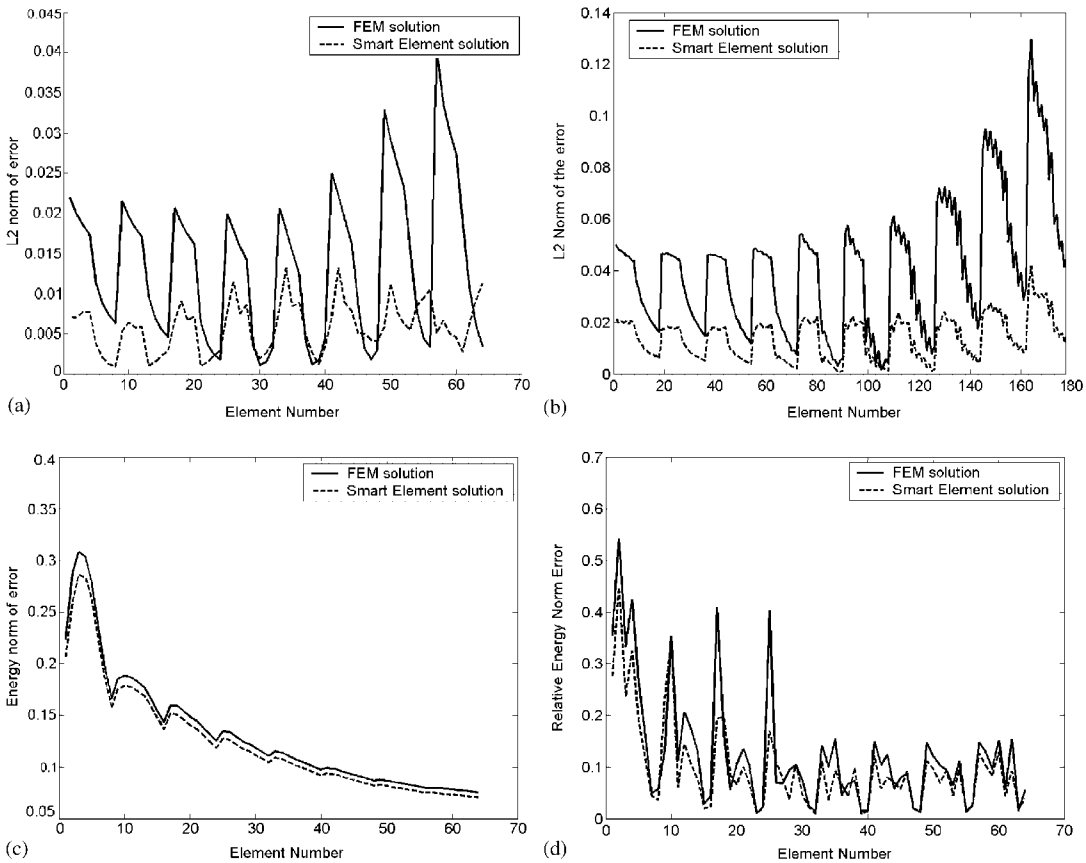

Figure 8. Element-wise error norm plots: (a) error L_2 norm, quadrilateral element; (b) error L_2 norm, triangle element; (c) error energy norm, quadrilateral element; and (d) error energy norm, triangle element.

Figures 10(a) and (b) show the convergence results. The volumetric locking in the conventional FEM solution is clearly visible in the figures. The smart element solution, however, seems to be hardly affected by the incompressibility restrain, as the result shows good overall convergence rate. Please also note that in Figure 10(a), the convergence plot of the smart element method is 'jagged'. In some region, increasing the number of elements will not lead to a big improvement in the accuracy. The detailed explanation and discussion about the performance of the smart element method dealing with volumetric locking will be the subject of later work. Shown in Figures 10(c) and (d) is the volume change of each element, which is calculated by $\Delta V = \varepsilon_{ii} = \varepsilon_{11} + \varepsilon_{22}$. Triangular elements are used in both cases. Figure 10(c) is computed with $\nu = 0.49$ and Figure 10(d) is computed with $\nu = 0.499$. We can see the smart element method solution preserve the volume satisfactorily as $\nu \to 0.5$. Overall the smart element method performs well in the nearly incompressible case.

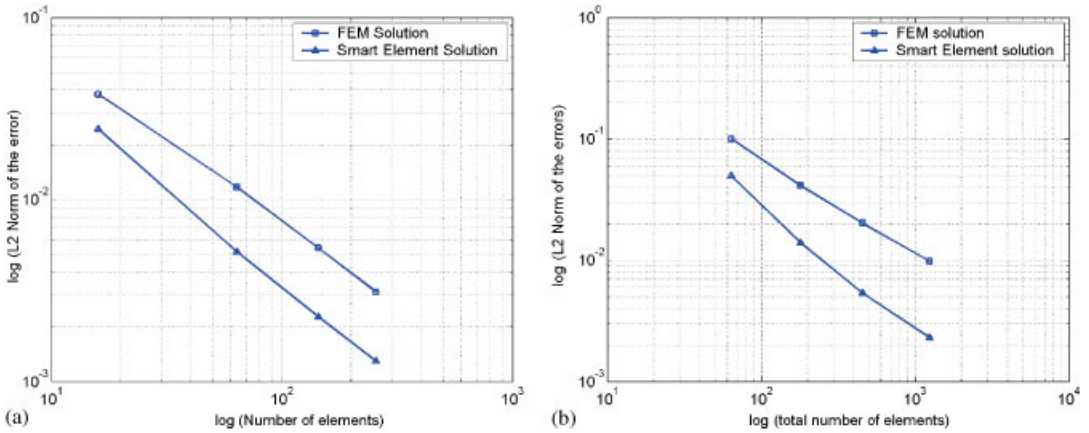

Figure 9. Convergence plots for the hole problem: (a) quadrilateral element; and (b) triangle element.

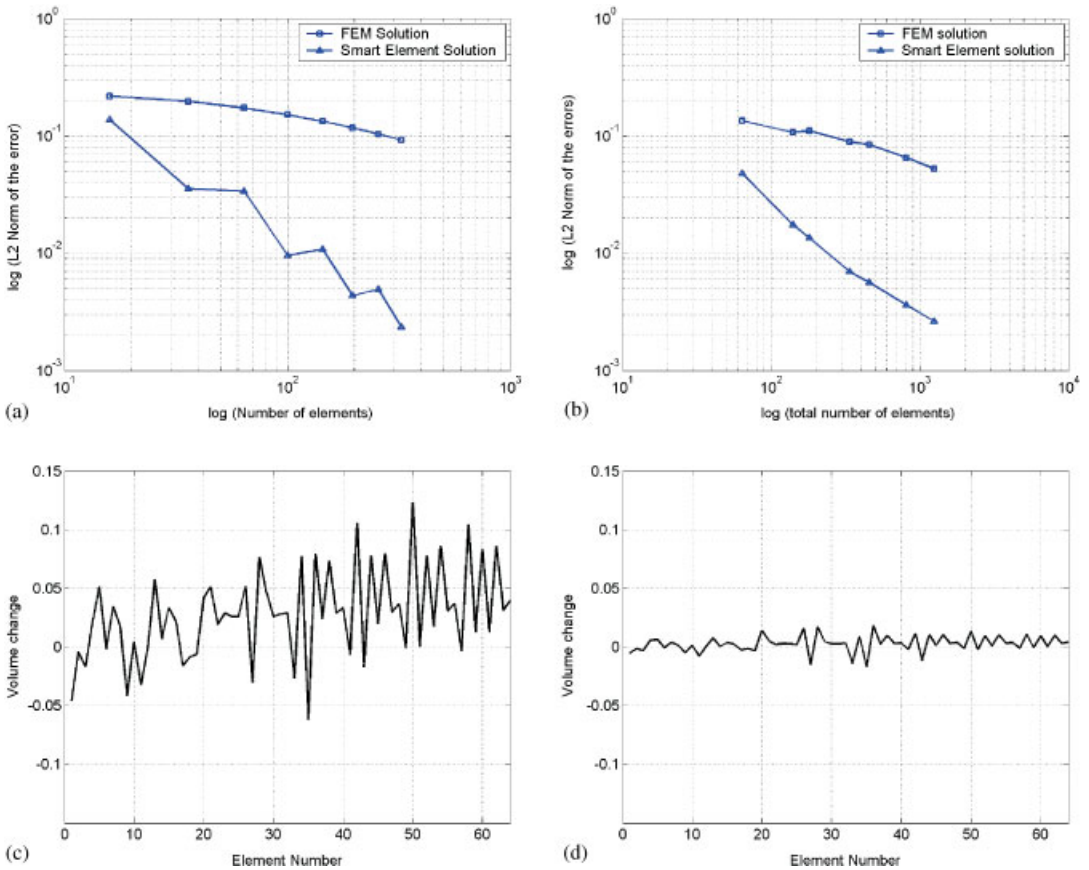

Figure 10. The nearly incompressible case: (a) log–log convergence plot with quadrilateral elements; (b) log–log convergence plot with triangular elements; (c) element-wise volume change, $\nu = 0.49$; and (d) element-wise volume change, $\nu = 0.499$.

6. CONCLUDING REMARKS

In this work, a new variational eigenstrain multiscale formulation is proposed to construct a homogenized two-scale variational weak formulation for elastostatics. The newly proposed FEM weak formulation combines Hughes' variational multiscale method, Eshelby's eigenstrain/inclusion theory, and the Zienkiewicz–Zhu *a posteriori* error estimator to control the discretization error automatically. Because it has the ability of self-adjustment, the smart element renders better computational performance in numerical computations than the conventional finite element for the same coarse scale computations. Preliminary numerical results show that the method provides better accuracy than regular finite element computations that have no homogenization of discretization error. We have consistently observed a 25% improvement in all numerical results obtained so far.

The traditional finite error estimations can be divided into two categories: (1) *A priori* error estimate, and (2) *A posteriori* error estimate. To the best of authors' knowledge, none of these error estimators has been incorporated into a feedback mechanism to adjust the original weak formulation. The variational multiscale formulation provides a perfect platform to utilize *a posteriori* error estimate of a coarse scale solution as the feedback signal. By combining it with Eshelby tensor (signal amplifier), and a proper recovery solution (e.g. the Zienkiewicz–Zhu correction in this paper), one can obtain a significant improvement in the accuracy of a coarse scale numerical solution, and achieve optimal correction by minimizing discretization error.

We are currently extending the smart element method to 3D elasticity problems, 2D Stokes flow problem and 2D advection–diffusion problems, studying its convergence criterion, and applying it to solve some pathological problems existing in traditional finite element literature, such as volumetric and shear locking problems.

APPENDIX A. TENSORS $S_{ijk\ell}$ OF 2D ELASTOSTATICS

The Green's function for 2D Navier equations is given as (e.g. Reference [23])

$$G_{ij}^{\infty}(\mathbf{y}-\mathbf{x}) = \frac{1}{8\pi\mu(1-\nu)}\left\{\frac{(y_i-x_i)(y_j-x_j)}{R^2} - (3-4\nu)\delta_{ij}\ln R\right\} \tag{A1}$$

where $i, j = 1, 2$ and $R = \sqrt{(y_2-x_2)^2+(y_1-x_1)^2}$.

It can be readily shown that

$$G_{ij,\ell}^{\infty}(\mathbf{y}-\mathbf{x}) = \frac{1}{8\pi\mu(1-\nu)}\left\{-2\frac{z_i z_j z_\ell}{R^4} + \frac{1}{R^2}(z_j\delta_{i\ell}+z_i\delta_{j\ell}) - (3-4\nu)\delta_{ij}\frac{z_\ell}{R^2}\right\}$$

where $\mathbf{z} = \mathbf{y} - \mathbf{x}$.

For isotropic materials,

$$C_{ijkl} = \lambda\delta_{ij}\delta_{k\ell} + \mu(\delta_{ik}\delta_{j\ell}+\delta_{jk}\delta_{i\ell})$$

Then, one can show that

$$C_{mnk\ell}G_{im,n}^{\infty}(\mathbf{z}) = -\frac{1}{4\pi(1-\nu)}\left\{2\frac{z_i z_k z_\ell}{R^4} + \frac{(1-2\nu)}{R^2}(z_k\delta_{i\ell}+z_\ell\delta_{ik}-z_i\delta_{k\ell})\right\}$$

Let,

$$\ell = -\frac{\mathbf{z}}{|\mathbf{z}|} = \frac{\mathbf{x}-\mathbf{y}}{|\mathbf{z}|} \tag{A2}$$

We may write

$$C_{mnk\ell} G^{\infty}_{im,n}(\mathbf{z}) = \frac{g_{ik\ell}(\boldsymbol{\ell})}{4\pi(1-\nu)|\mathbf{z}|} \tag{A3}$$

where

$$g_{ik\ell}(\boldsymbol{\ell}) = 2\ell_i\ell_k\ell_\ell + (1-2\nu)(\ell_k\delta_{i\ell} + \ell_\ell\delta_{ik} - \ell_i\delta_{k\ell}) \tag{A4}$$

Let $|\mathbf{z}| = R$ then for $\mathbf{y} \in \Omega_e$ the integration,

$$\int_{\Omega_e^c} C_{mnk\ell} G^{\infty}_{im,n}(\mathbf{z})\,\mathrm{d}\Omega = \frac{1}{4\pi(1-\nu)} \int_0^r \left(\int_0^{2\pi} \frac{g_{ik\ell}(\boldsymbol{\ell})}{R}\,\mathrm{d}\omega \right) R\,\mathrm{d}R \tag{A5}$$

is carried out in the circle, Ω_e^c.

Here $x_1 = y_1 + r\ell_1$ and $x_2 = y_2 + r\ell_2$. Since

$$x_1^2 + x_2^2 = a^2 \Rightarrow (y_1 + r\ell_1)^2 + (y_2 + r\ell_2)^2 = a^2$$

where r is the root of the following quadratic equation:

$$r^2 + 2r(y_1\ell_1 + y_2\ell_2) + [a^2 - (y_1^2 + y_2^2)] = 0 \rightarrow r^2 + 2rf - e = 0 \tag{A6}$$

where $f = \ell_i y_i$ and $e = a^2 - (y_1^2 + y_2^2)$. The roots of Equation (A6) are

$$r(\boldsymbol{\ell}) = -f \pm \sqrt{f^2 + e}$$

Considering $\sqrt{f^2+e}$ is an even function of $\boldsymbol{\ell}$. We have (Figure A1)

$$\int_{\Omega_e^c} C_{mnk\ell} G^{\infty}_{im,n}(\mathbf{z})\,\mathrm{d}\Omega = \frac{-y_s}{4\pi(1-\nu)} \int_0^{2\pi} \ell_s g_{ik\ell}(\boldsymbol{\ell})\,\mathrm{d}\theta \tag{A7}$$

Therefore,

$$\begin{aligned} S_{ijk\ell} &= -\frac{1}{2} \int_{\Omega_e^c} C_{mnk\ell} (G^{\infty}_{im,nj}(\mathbf{z}) + G^{\infty}_{jm,ni}(\mathbf{z}))\,\mathrm{d}\Omega_x \\ &= \frac{1}{8\pi(1-\nu)} \int_0^{2\pi} (\ell_j g_{ik\ell}(\boldsymbol{\ell}) + \ell_i g_{jk\ell}(\boldsymbol{\ell}))\,\mathrm{d}\theta \end{aligned} \tag{A8}$$

Using the identities (e.g. Reference [24]),

$$\int_0^{2\pi} \ell_i\ell_j\,\mathrm{d}\theta = \pi\delta_{ij} \tag{A9}$$

$$\int_0^{2\pi} \ell_i\ell_j\ell_k\ell_\ell\,\mathrm{d}\theta = \frac{\pi}{4}(\delta_{ij}\delta_{k\ell} + \delta_{ik}\delta_{j\ell} + \delta_{i\ell}\delta_{jk}) \tag{A10}$$

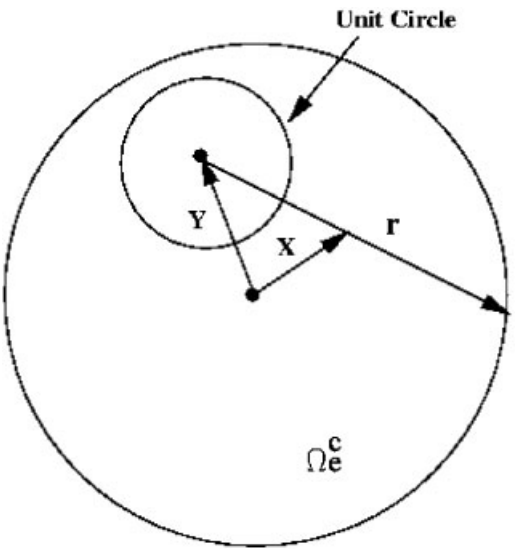

Figure A1.

One can obtain,

$$S_{ijk\ell} = \frac{1}{8(1-\nu)}((4\nu-1)\delta_{ij}\delta_{k\ell} + (3-4\nu)(\delta_{ik}\delta_{j\ell} + \delta_{i\ell}\delta_{jk}) \tag{A11}$$

$$= \frac{1}{2(1-\nu)} E^{(1)}_{ijk\ell} + \frac{(3-4\nu)}{4(1-\nu)} E^{(2)}_{ijk\ell} \tag{A12}$$

APPENDIX B. DERIVATION OF EQUATION (44)

Consider

$$u'_i(\mathbf{y}) = \int_{\Omega_e^c} C_{mnk\ell}(\bar{u}_{(k,\ell)}(\mathbf{x}) - u_{(k,\ell)}(\mathbf{x}))G^{\infty}_{im,n}(\mathbf{y}-\mathbf{x})\,\mathrm{d}\Omega_x \tag{B1}$$

By differentiation (B1), we obtain the expression of the fine scale strain,

$$\varepsilon'_{ij}(\mathbf{y}) = \int_{\Omega_e^c} \tfrac{1}{2} C_{mnk\ell}(\bar{u}_{(k,\ell)}(\mathbf{x}) - u_{(k,\ell)}(\mathbf{x}))(G^{\infty}_{im,nj}(\mathbf{y}-\mathbf{x}) + G^{\infty}_{jm,ni}(\mathbf{y}-\mathbf{x}))\,\mathrm{d}\Omega_x \tag{B2}$$

Define $\bar{u}_{(k,\ell)} - u_{(k,\ell)}$ as eigenstrain:

$$\varepsilon^*_{k\ell}(\mathbf{x}) = u_{(k,\ell)}(\mathbf{x}) - \bar{u}_{(k,\ell)}(\mathbf{x}) \tag{B3}$$

The Taylor series expansion of ϵ^* at $\mathbf{y}$ can be written as

$$\varepsilon^*_{k\ell}(\mathbf{x}) = \sum_{|\alpha|=0}^{\infty} \frac{1}{\alpha!} D^{\alpha} \varepsilon^*_{k\ell}(\mathbf{y})(\mathbf{x}-\mathbf{y})^{\alpha} \tag{B4}$$

where $\alpha = (\alpha_1, \ldots, \alpha_d)$ is the d-dimensional multi-index. For the 3D case, we can re-write it in component form

$$\varepsilon^*_{k\ell}(\mathbf{x}) = \sum_{p+q+r=0}^{\infty} \varepsilon^*_{k\ell pqr}(\mathbf{y}) x_1^p x_2^q x_3^r \tag{B5}$$

Rahman [25] shows that with the above polynomial expression of the eigenstrain, the resulted displacement field has the following form:

$$u'_i(\mathbf{y}) = \eta_1 \partial_i \Gamma^N_{mm} - \eta_2 \partial_j \Gamma^N_{ij} + \eta_3 \bar{y}_k \partial_i \partial_j \Gamma^N_{jk} - \eta_3 a \partial_i \partial_j \ {}^{(k)}\tilde{\Gamma}^N_{jk} \tag{B6}$$

where η_i are dimensionless coefficients and a is the radius of Ω^c_e. We can then obtain the strain expression:

$$\begin{aligned} \varepsilon'_{i\ell}(\mathbf{y}) = {} & \eta_1 \partial_i \partial_\ell \Gamma^N_{mm} - \tfrac{1}{2}\eta_2(\partial_j \partial_\ell \Gamma^N_{ij} + \partial_j \partial_i \Gamma^N_{\ell j}) + \tfrac{1}{2}\eta_3(\partial_i \partial_j \Gamma^N_{j\ell} + \partial_\ell \partial_j \Gamma^N_{ji}) \\ & + \eta_3 \bar{y}_k \partial_i \partial_j \partial_\ell \Gamma^N_{jk} - \eta_3 a \partial_i \partial_j \partial_\ell \ {}^{(k)}\tilde{\Gamma}^N_{jk} \end{aligned} \tag{B7}$$

the Γ_{ij} and $\tilde{\Gamma}_{ij}$ are given by Rahman as

$$\Gamma^N_{ij} = \sum_{p+q+r=0}^{N+2} F^{ij}_{pqr} \bar{y}_1^p \bar{y}_2^q \bar{y}_3^r \tag{B8}$$

$${}^{(k)}\tilde{\Gamma}^N_{ij} = \sum_{p+q+r=0}^{N+3} {}^{(k)}\tilde{F}^{ij}_{pqr} \bar{y}_1^p \bar{y}_2^q \bar{y}_3^r \tag{B9}$$

The N here is the order of the polynomial in (B5). $\bar{\mathbf{y}}$ is the local co-ordinate. The expressions for F^{ij}_{pqr} and ${}^{(k)}\tilde{F}^{ij}_{pqr}$ can be find in Reference [25]. For the interior solution, they can be written in a compact form:

$$F^{ij}_{pqr} = c_{ijpqr}(\mathbf{y}) a^{-p-q-r} \tag{B10}$$

$${}^{(k)}\tilde{F}^{ij}_{pqr} = \tilde{c}_{ijpqr}(\mathbf{y}) a^{-p-q-r} \tag{B11}$$

where c_{ijpqr} and $\tilde{c}_{ijpqr}$ are derivatives of the eigenstrain ε^*_{ij} (See (B4) and (B5)). They are dimensionless.

Substitute (B10) and (B11) into (B8) and (B9), we obtain

$$\Gamma^N_{ij} = \sum_{p+q+r=0}^{N+2} c_{ijpqr} \left(\frac{\bar{y}_1}{a}\right)^p \left(\frac{\bar{y}_2}{a}\right)^q \left(\frac{\bar{y}_3}{a}\right)^r \tag{B12}$$

$$ {}^{(k)}\tilde{\Gamma}_{ij}^{N} = \sum_{p+q+r=0}^{N+3} \tilde{c}_{ijpqr} \left(\frac{\bar{y}_1}{a}\right)^p \left(\frac{\bar{y}_2}{a}\right)^q \left(\frac{\bar{y}_3}{a}\right)^r \tag{B13} $$

Notice that $\bar{y}_k/a$ is smaller than one, so its powers are small. Thus the above equations can be written as

$$ \Gamma_{ij}^{N} = \sum_{p+q+r=0}^{2} c_{ijpqr} \left(\frac{\bar{y}_1}{a}\right)^p \left(\frac{\bar{y}_2}{a}\right)^q \left(\frac{\bar{y}_3}{a}\right)^r + \mathcal{O}\left(\left(\frac{\bar{y}_k}{a}\right)^3\right) \tag{B14} $$

$$ {}^{(k)}\tilde{\Gamma}_{ij}^{N} = \sum_{p+q+r=0}^{3} \tilde{c}_{ijpqr} \left(\frac{\bar{y}_1}{a}\right)^p \left(\frac{\bar{y}_2}{a}\right)^q \left(\frac{\bar{y}_3}{a}\right)^r + \mathcal{O}\left(\left(\frac{\bar{y}_k}{a}\right)^4\right) \tag{B15} $$

For the exterior solution, the expressions of F_{ijk} and $\tilde{F}_{ijk}$ change to

$$ F_{pqr}^{ij} = c_{ijpqr} R^{-p-q-r} \tag{B16} $$

$$ {}^{(k)}\tilde{F}_{pqr}^{ij} = \tilde{c}_{ijpqr} R^{-p-q-r} \tag{B17} $$

where $R = |\bar{\mathbf{y}}|$. Then (B8) and (B9) become:

$$ \Gamma_{ij}^{N} = \sum_{p+q+r=0}^{N+2} c_{ijpqr} \left(\frac{\bar{y}_1}{R}\right)^p \left(\frac{\bar{y}_2}{R}\right)^q \left(\frac{\bar{y}_3}{R}\right)^r \tag{B18} $$

$$ {}^{(k)}\tilde{\Gamma}_{ij}^{N} = \sum_{p+q+r=0}^{N+3} \tilde{c}_{ijpqr} \left(\frac{\bar{y}_1}{R}\right)^p \left(\frac{\bar{y}_2}{R}\right)^q \left(\frac{\bar{y}_3}{R}\right)^r \tag{B19} $$

$\bar{y}_k/R$ is smaller than one, so similar to the interior case, we can write (B18) and (B19) as

$$ \Gamma_{ij}^{N} = \sum_{p+q+r=0}^{2} c_{ijpqr} \left(\frac{\bar{y}_1}{R}\right)^p \left(\frac{\bar{y}_2}{R}\right)^q \left(\frac{\bar{y}_3}{R}\right)^r + \mathcal{O}\left(\left(\frac{\bar{y}_k}{R}\right)^3\right) \tag{B20} $$

$$ {}^{(k)}\tilde{\Gamma}_{ij}^{N} = \sum_{p+q+r=0}^{3} \tilde{c}_{ijpqr} \left(\frac{\bar{y}_1}{R}\right)^p \left(\frac{\bar{y}_2}{R}\right)^q \left(\frac{\bar{y}_3}{R}\right)^r + \mathcal{O}\left(\left(\frac{\bar{y}_k}{R}\right)^4\right) \tag{B21} $$

So in both cases, we can neglect the higher order terms, i.e.

$$ \Gamma_{ij}^{N} \approx \sum_{p+q+r=0}^{2} c_{ijpqr} \left(\frac{\bar{y}_1}{a}\right)^p \left(\frac{\bar{y}_2}{a}\right)^q \left(\frac{\bar{y}_3}{a}\right)^r \tag{B22} $$

$$ {}^{(k)}\tilde{\Gamma}_{ij}^{N} \approx \sum_{p+q+r=0}^{3} \tilde{c}_{ijpqr} \left(\frac{\bar{y}_1}{a}\right)^p \left(\frac{\bar{y}_2}{a}\right)^q \left(\frac{\bar{y}_3}{a}\right)^r \tag{B23} $$

for the interior case, and

$$\Gamma_{ij}^{N} \approx \sum_{p+q+r=0}^{2} c_{ijpqr} \left(\frac{\bar{y}_1}{R}\right)^p \left(\frac{\bar{y}_2}{R}\right)^q \left(\frac{\bar{y}_3}{R}\right)^r \tag{B24}$$

$$^{(k)}\tilde{\Gamma}_{ij}^{N} \approx \sum_{p+q+r=0}^{3} \tilde{c}_{ijpqr} \left(\frac{\bar{y}_1}{R}\right)^p \left(\frac{\bar{y}_2}{R}\right)^q \left(\frac{\bar{y}_3}{R}\right)^r \tag{B25}$$

for the exterior case. This is equivalent to only keep the constant term in (B4), i.e. choose $N = 0$ instead of $N = \infty$.

We can then replace $\varepsilon^*_{k\ell}(\mathbf{x})$ by $\varepsilon^*_{k\ell}(\mathbf{y})$ in (B2), and

$$\begin{aligned}
\varepsilon'_{ij}(\mathbf{y}) &= -\int_{\Omega_e^c} \tfrac{1}{2} C_{mnk\ell} \varepsilon^*_{k\ell}(\mathbf{x}) (G^{\infty}_{im,nj}(\mathbf{y}-\mathbf{x}) + G^{\infty}_{jm,ni}(\mathbf{y}-\mathbf{x}))\, \mathrm{d}\Omega_x \\
&\approx -\int_{\Omega_e^c} \tfrac{1}{2} C_{mnk\ell} \varepsilon^*_{k\ell}(\mathbf{y}) (G^{\infty}_{im,nj}(\mathbf{y}-\mathbf{x}) + G^{\infty}_{jm,ni}(\mathbf{y}-\mathbf{x}))\, \mathrm{d}\Omega_x \\
&= S_{ijk\ell} \varepsilon^*_{k\ell}(\mathbf{y}).
\end{aligned} \tag{B26}$$

This is the desired expression.

The above derivation is done for the 3D case, which includes the 2D problem as a special case.

ACKNOWLEDGEMENTS

The authors would like to thank the anonymous referees for their constructive comments and suggestions. We would also like to thank Ashutosh Agrawal for his useful help.

This work is made possible by a NSF grant (Grant No. CMS-0239130 to University of California at Berkeley), which is greatly appreciated.

REFERENCES

1. Li S, Gupta A, Liu X, Mahyari M. Variational eigenstrain multiscale finite element method. *Computer Methods in Applied Mechanics and Engineering* 2004; **193**:1803–1824.
2. Cantin G, Loubignac C, Touzot C. An iterative scheme to build continuous stress and displacement solutions. *International Journal for Numerical Methods in Engineering* 1978; **12**:1493–1506.
3. Eshelby JD. The elastic field outside an ellipsoidal inclusion. *Proceedings of Royal Society of London* 1957; **A252**:561–569.
4. Eshelby JD. The elastic field outside an ellipsoidal inclusion. *Proceedings of Royal Society of London* 1959; **A252**:561–569.
5. Eshelby JD. Elastic inclusions and inhomogeneities. In *Progress in Solid Mechanics*, Sneddon IN, Hill R (eds), vol. 2. North-Holland: Amsterdam, 1961; 89–140.
6. Sanchez-Palencia E. *Non-Homogeneous Media and Vibration Theory*. Lecture Notes in Physics, vol. 127. Springer: Berlin, 1980.
7. Guedes JM, Kikuchi N. Preprocessing and postprocessing for materials based on the homogenization method with adaptive finite element methods. *Computer Methods in Applied Mechanics and Engineering* 1990; **83**: 143–198.

8. Tong P, Mei CC. Mechanics of composite of multiple scales. *Computational Mechanics* 1992; **9**:195–201.
9. Zienkiewicz OC, Zhu JZ. A simple error estimator and adaptive procedure for practical engineering analysis. *International Journal for Numerical Methods and Analysis* 1987; **24**:337–357.
10. Zienkiewicz OC, Zhu JZ. The superconvergent patch recovery and *a posteriori* error estimates: Part I. The recovery technique. *International Journal for Numerical Methods in Engineering* 1992a; **33**:1331–1364.
11. Zienkiewicz OC, Zhu JZ. The superconvergent patch recovery and *a posteriori* error estimates: Part II. Error estimates and adaptivity. *International Journal for Numerical Methods and Engineering* 1992b; **33**: 1365–1382.
12. Hughes TJR. Multiscale phenomena: Green's functions, the Dirichlet-to-Neumann formulation, subgrid scale models, bubbles and the origins of stabilized methods. *Computer Methods in Applied Mechanics and Engineering* 1995; **127**:387–401.
13. Hughes TJR, Stewart J. A space–time formulation for multiscale phenomena. *Journal of Computational Applied Mathematics* 1996; **74**:217–229.
14. Hughes TJR, Feijoo GR, Mazzei L, Quincy J-B. The variational multiscale method—a paradigm for computational mechanics. *Computer Methods in Applied Mechanics and Engineering* 1998; **166**:3–24.
15. Adams RA. *Sobolev Spaces*. Academic Press: New York, San Francisco, London, 1975.
16. Brenner SC, Scott LR. *The Mathematical Theory of Finite Element Methods*. Springer: New York, 1994.
17. Renardy M, Rogers RC. *An Introduction to Partial Differential Equations*. Springer: New York, Berlin, 1993.
18. Mura T. *Micromechanics of Defects in Solids*. Martinus Nijhoff Publishers: Dordrecht, 1987.
19. Somigliana C. Sopra l'equilibrio di un corpo elastico isotropo. *Nuovo Ciemento* 1885; **17**:140–148.
20. Hughes TJR. *The Finite Element Method*. Prentice-Hall: Englewood Cliffs, NJ, 1987.
21. Timoshenko SP, Goodier JN. *Theory of Elasticity* (3rd edn). McGraw-Hill: New York, 1970.
22. Zienkiewicz OC, Taylor RL. *The Finite Element Method*, *vol. 1. The Basis* (5th edn). Butterworth-Heinemann: London, 2000.
23. Brebbia CA, Walker S. *Boundary Element Techniques in Engineering*. Newnes-Butterworths: London, Boston, 1980.
24. Krajcinovi D. *Damage Mechanics*. Elsevier: Amsterdam, New York, 1996.
25. Rahman M. The isotropic ellipsoidal inclusion with a polynomial distribution of eigenstrain. *Journal of Applied Mechanics* (ASME) 2002; **69**:593–601.

